

University of Alberta

**ROLE OF GLUTAMATE AND GABA IN A MOUSE MODEL
EXPRESSING MUTANT HUMAN APP IN THE ABSENCE OF NPC1
PROTEIN**

by

BIBASWAN GHOSHAL

A thesis submitted to the Faculty of Graduate Studies and Research
in partial fulfillment of the requirements for the degree of

Master of Science

Department of Psychiatry

©Bibaswan Ghoshal

Spring 2013

Edmonton, Alberta

Permission is hereby granted to the University of Alberta Libraries to reproduce single copies of this thesis and to lend or sell such copies for private, scholarly or scientific research purposes only. Where the thesis is converted to, or otherwise made available in digital form, the University of Alberta will advise potential users of the thesis of these terms.

The author reserves all other publication and other rights in association with the copyright in the thesis and, except as herein before provided, neither the thesis nor any substantial portion thereof may be printed or otherwise reproduced in any material form whatsoever without the author's prior written permission.

ABSTRACT

Cholesterol plays a critical role in Alzheimer's disease (AD) pathogenesis, but the underlying mechanisms remain unclear. To address this issue we have generated a line of ANPC transgenic mice that overexpress mutant-human amyloid precursor protein in the absence of cholesterol transporting Niemann Pick-type C1 protein. These mice display accelerated AD-related pathology compared to age-matched littermates. To define significance of GABA and glutamate in AD, we evaluated alterations of these systems in ANPC mice at different age groups. The levels of glutamate and GABA were not unaltered in ANPC mice compared to other lines. However, levels of vesicular glutamate transporter 1 (i.e. VGLUT1), and expression of VGLUT1 and VGLUT2 appeared to be decreased in ANPC mice. The levels/distribution of glutamic acid decarboxylase 67 (i.e. GAD67) but not GAD65 were also decreased in the cerebellum of ANPC mice. Thus, cholesterol accumulation influences AD-related pathology and triggers subtle alterations in brain neurotransmitter system.

ACKNOWLEDGEMENTS

I am deeply indebted to all individuals who have assisted and supported me in this endeavor. The guidance, indulgence, and encouragement I received from them are deeply appreciated.

I would like to extend my sincere thanks to my supervisor, Dr. Satyabrata Kar, for his enormous supervision, guidance and support in the past two years. It would have been impossible for me to complete this daunting task without the advice and inspiration provided by him. Dr. Glen Baker and Dr. Jean Michel LeMelledo deserve special thanks as my thesis committee members and advisors. I would also like to thank to all of the people who helped me in the lab during past two years, specifically Ms. Mahua Maulik, Ms. Ronke Babatunde, Dr. Timothy Revett, Mr. Robert Mercer, Mr. Yanlin Wang, Dr. Hariharakrishnan Janaradhanan, Ms. Anitha Kodam, and Dr. Asha Amritraj. I would also like to extend a special thanks to Ms. Mahua Maulik who has been my mentor all through and helped me out not only as a lab member but as a part of my family. As well, I like to thank Dr. Glen Baker and Ms. Gail Rauw from the Neurochemical Research Unit, Department of Psychiatry for their help and technical advice with the HPLC. I would also like to pay my gratitude to CIHR for the financial support for this research.

I would also like to thank members from the Westaway Lab, specially, Dr. Jing Yang, Dr. David Vergotte, Ms. Agnes Lau and Dr. Laura Edwards-Ingram for their positive inputs and advice for my project, and also to all the members of Centre for Prions and Protein Folding Diseases for their never ending love and support.

I am grateful to Mr. Advaita Ganguly, Mr. Kaustav Majumdar and Mr. Anirban Chakrabarty, who has been not only been my brother but also friend, philosopher and guide in these critical years of my life. I am thankful to Mr. Debmalya Mukherjee, Mrs. Sarmita Mukherjee and Debdeep Mukherjee for their support and love; I regard them as my family. They all make me feel Edmonton is my second home and help me survive the harsh Edmonton weather. I would also like to thank the following people for their support and encouragement: Dr. Moulinath

Acharya, Bijoyendra Bera, Reeshav Chatterjee, Dr. Jitendra Kumar, Dr. Mayukh Banerjee, Subhadyuti Chanda, Anindyo Ghosh, Dr. Arghya Basu, and Dr. Paramita Chaudhuri. I am extremely thankful to my parents Bidhan Chandra Ghoshal and Baisali Ghoshal, my grandmother Kalyani Mukherjee, my uncle Gobin Boral, my wife Angana Samanta and all my family members and friends from India for their encouragement and support.

Last, but not least, I am deeply indebted to my late grandfather, Shri Samir Mukherjee and Swami Vivekananda, whose ideology and thoughts help me throughout my life. Without that, I would never have come this far.

TABLE OF THE CONTENTS

CHAPTER – 1

General Introduction and Literature Review

1.1 Alzheimer's Disease (AD)	1
1.2 Cholesterol and AD	4
1.3 Niemann Pick Type C (NPC) Disease	6
1.4 Glutamate and its role in AD and NPC Disease	7
1.5 GABA and its role in AD and NPC Disease	10
1.6 Hypothesis	12

CHAPTER – 2

Materials and Methods

2.1 Materials	14
2.2 Animals	14
2.3 DNA analysis	15
2.4 Tissue collection	16
2.5 Western blotting	16
2.6 Immunohistochemistry	17
2.7 High Performance Liquid Chromatography (HPLC)	18
2.7.1 Apparatus	18
2.7.2 Chemicals and reagents	18
2.7.3 Chromatographic conditions	18
2.7.4 Derivatization procedure	19
2.7.5 Standards and sample preparation for HPLC	19
2.8 Data analysis	19

CHAPTER – 3

Results

3.1 Determination of glutamate and GABA levels in the frontal cortex and cerebellum of ANPC mice	20
3.2 Determination of glutamatergic and GABAergic markers in the frontal cortex and cerebellum of ANPC mice	20
3.3 Distribution profile of the glutamatergic and GABAergic markers in ANPC mice	23

CHAPTER – 4

Discussion	45
References	53

LIST OF TABLES

Table 1. List of mouse genotypes

16

LIST OF FIGURES

Figure 1. HPLC data on glutamate in the frontal cortex and cerebellum	26
Figure 2. HPLC data on GABA in the frontal cortex and cerebellum	27
Figure 3. Western blots and quantification of VGLUT1 in the frontal cortex	28
Figure 4. Western blots and quantification of VGLUT1 in the cerebellum	29
Figure 5. Western blots and quantification of VGLUT2 in the frontal cortex	30
Figure 6. Western blots and quantification of VGLUT2 in the cerebellum	31
Figure 7. Western blots and quantification of GAD65 in the frontal cortex	32
Figure 8. Western blots and quantification of GAD65 in the cerebellum	33
Figure 9. Western blots and quantification of GAD67 in the frontal cortex	34
Figure 10. Western blots and quantification of VGLUT1 in the cerebellum	35
Figure 11. Immunohistochemistry of VGLUT1 and NeuN at 4 weeks in frontal cortex	36
Figure 12. Immunohistochemistry of VGLUT1 and NeuN at 10 weeks in frontal cortex	37
Figure 13. Immunohistochemistry of VGLUT2 and NeuN at 4 weeks in frontal cortex	38

Figure 14. Immunohistochemistry of VGLUT2 and NeuN at 10 weeks in frontal cortex	39
Figure 15. Immunohistochemistry of GAD65 and NeuN at 4 weeks in frontal cortex	40
Figure 16. Immunohistochemistry of GAD65 and NeuN at 10 weeks in frontal cortex	41
Figure 17. Immunohistochemistry of GAD67 and NeuN at 4 weeks in frontal cortex	42
Figure 18. Immunohistochemistry of GAD67 and NeuN at 10 weeks in frontal cortex	43
Figure 19. Immunohistochemistry of VGLUT1 and Calbindin D-28k at 4 and 10 weeks in cerebellum	44
Figure 20. Immunohistochemistry of VGLUT2 and Calbindin D-28k at 4 and 10 weeks in cerebellum	44

LIST OF ABBREVIATIONS

a.a	amino acid
A β	Amyloid β peptide
AD	Alzheimer's disease
AMPA	α -amino-3-hydroxy-5-methyl-4-isoxazole propionate
APOE	Apolipoprotein E
APP	Amyloid precursor protein
APP-Tg	APP-Transgenic
BSA	Bovine serum albumin
BACE	β -site APP cleaving enzyme
CNS	Central nervous system
Dhet	Double heterozygous
EAAT	Excitatory amino acid transporters
ECL	Enhanced chemiluminescence
E/L	Endosomal/Lysosomal
EOAD	Early onset Alzheimer's Disease
ER	Endoplasmic reticulum
FC	Frontal cortex
FITC	Fluorescein isothiocyanate
GABA	γ -aminobutyric acid
GAD	Glutamic acid decarboxylase
GAT	GABA transporter
GluR	Glutamate receptor

GS	Glutamate synthetase
HDL	High density lipoprotein
HMG-CoA	3-hydroxy-3-methyl-glutaryl coenzyme A
KA	Kainic acid
kD	kiloDalton
LDL	Low density lipoprotein
LOAD	Late onset Alzheimer's Disease
NFT	Neurofibrillary tangles
NMDA	N-methyl-D-aspartate
NP	Neuritic plaques
NPC	Niemann Pick Type C
NPC1-ko	Niemann Pick type C-1 knock out
PBS	Phosphate-buffered saline
PHF	Paired helical filaments
PNS	Peripheral nervous system
PSEN1/PSEN2	Presenilin1/Presenilin 2
SREBP	Sterol-regulatory element binding protein
SSD	Sterol-sensing domain
TCA	Tricarboxylic Acid
WT	Wild-type
VGAT	Vesicular GABA transporter
VGLUT	Vesicular glutamate transporter
VLDL	Very low density lipoprotein

1. Introduction

1.1 Alzheimer's Disease: Alzheimer's disease (AD) is an age-related neurodegenerative disorder that leads to a chronically progressive decline in cognitive functions. Several studies across the globe have identified AD as an immense social and economic burden (Alloul et al., 1998). According to the World Alzheimer Report 2010, submitted by AD International, the total cost of dementia is US \$604 billion worldwide in 2010 and tentatively estimated to increase by 85% until 2030. AD is the most common form of dementia, accounting for 50-56% of all cases of dementia at autopsy. This neurodegenerative disease is characterized by a progressive cognitive decline and a loss of memory. The capacity to recall not only recent events, but also to learn and retain new information, is severely affected. Reasoning ability and spatial and visuo-perceptual ability are also impaired, accompanied by language deficits and changes in behavior (Grabowski & Damasio, 1996). The major risk factor for AD is age. Between 65 and 74 years of age, ~1.6% of the US population is affected by AD, while ~43% is affected above the age of 85 years (Hebert et al., 2003).

The majority (90-95%) of AD cases are non-familial, "sporadic" cases of late (\geq 65 years) onset (LOAD), whereas the inherited forms of AD, with an early disease onset (EOAD), account for as low as 5-10% of all cases. Phenotypic analyses have shown that these two variants of AD have a strong similarity and are indistinguishable with regard to symptoms (Mancuso et al., 2006; Selkoe, 2001). To date, all EOAD cases are known to be caused by mutations in three genes: Amyloid precursor protein (APP), Presenilin 1 (PSEN1) and Presenilin 2 (PSEN2). Mutations in the PSEN1 gene have been reported to account for up to 55% of the known EOAD cases (Lleo et al., 2002; Murphy et al., 2003). The APP gene is responsible for the formation of the APP protein, whereas the PSEN1 and PSEN2 genes are responsible for the generation of presenilin proteins which form

the core part of the γ -secretase complex, an enzyme involved in the generation of amyloid β ($A\beta$) peptide from APP.

The unequivocal diagnosis of AD relies, however, on the histopathological evidence at brain autopsy or biopsy. Primarily, the major pathological hallmarks of AD are the presence of $A\beta$ -containing neuritic plaques, tau-positive neurofibrillary tangles (NFTs), and loss of neurons in selected brain regions (Hardy & Selkoe, 2002). Neuritic plaques not only contain aggregates of $A\beta$ protein derived from APP (Esch et al., 1990; Sisodia et al., 1990), but also other proteins such as Apolipoprotein E (APOE) (Namba et al., 1991; Uchihara et al., 1995), growth factors, a variety of proteinases (such as trypsin) and proteinase inhibitors (Siman et al., 1993). Intact $A\beta$, which is proteolytically cleaved from its precursor protein APP by proteases referred to as β - and γ -secretases (Haass, 2004), occurs as 40 and 42 amino acid peptides ($A\beta_{1-40}$, $A\beta_{1-42}$) (Citron et al., 1996). In contrast to the amyloidogenic pathway, APP can also be cleaved by α -secretase *via* a non-amyloidogenic pathway which does not generate full-length $A\beta$ peptide. Plaques without abnormal neurites are called 'diffuse plaques', whereas those surrounded by abnormal dystrophic neurites are referred to as 'neuritic plaques'. Though the relationship between these two types of plaques is not entirely clear, one major difference is the length of $A\beta$ that is present. Diffuse plaques contain primarily $A\beta_{1-42}$ peptide, whereas neuritic plaques contain both $A\beta_{1-42}$ and $A\beta_{1-40}$ isoforms (Iwatsubo et al., 1994).

The three forms of neurofibrillary pathology present in AD brains include the NFTs, the dystrophic neurites of neuritic plaques and the neuropil threads (NTs) which are found scattered in the neuropil (Samuel et al., 1994). All represent accumulations of insoluble paired helical filaments (PHFs) which are composed of abnormally hyperphosphorylated microtubule-associated tau protein (Goedert, 1993). In pyramidal neurons, NFTs accumulate in the cytoplasm in a flame shape manner with displaced nucleus. The PHFs are so insoluble that they remain within

the neuropil as ghost tangles after the death and degeneration of the cell in which they developed (Yamaguchi et al., 1991).

While in normal human aging only neurons from the dentate hilus and from the subiculum die, there is evidence that neuronal density in the CA1 hippocampal region and layers II and IV of the entorhinal and other associated cortices are severely diminished in AD pathology (Gomez-Isla et al., 1996; Morrison & Hof, 1997b). At the subcortical level, the cholinergic neurons of the basal forebrain nucleus of Meynert and diagonal band of Broca are also severely affected, in parallel with reduced concentrations of acetylcholine (ACh) and acetylcholinesterase (AChE) activity in their projection zones, the hippocampus and the cortex (Davies & Maloney, 1976; Price et al., 1982). The synthesis of ACh is assured by a reaction of choline and acetyl co-enzyme A (acetyl Co-A) in the presence of enzyme, choline acetyltransferase (ChAT); the concentrations of ACh and the activity of ChAT are greatly diminished in the brain of AD patients compared to age-matched normal controls (Nitsch et al., 1992; Price et al., 1982).

Despite the low proportion of familial AD caused by gene mutations, their biological significance is important because they all result in an overall or selective increase in production of A β -related peptides, which are the primary components of amyloid deposition (Hardy, 1997; Tanzi et al., 1994). This finding, added to the fact that Down's syndrome patients develop AD pathology and possess an additional chromosome 21 where the APP gene is located, point to a role for A β in AD pathogenesis. This gave rise the amyloid cascade hypothesis first proposed by J.Hardy in 1991 as a possible pathological mechanism and summarized by D. Selkoe in 1997 as follows: *"all gene defects lead to enhanced production, increased aggregation, or perhaps decreased clearance of A β peptides. A β ₁₋₄₂, which is highly self-aggregating, would then accumulate, followed by A β ₁₋₄₀. The gradual cerebral build-up of A β appears to result in local microglial and astrocytic activation, with concomitant release of cytokines and acute phase proteins. These inflammatory changes or the direct toxicity of A β*

would injure local neurons and their processes, causing profound metabolic changes. These could include altered tau phosphorylation and PHF formation in some plaque-associated neurites and in neurons containing NFTs. Neuronal and glial injury would result in synaptic and neuronal loss, accompanied by several neurotransmitter deficits” (Selkoe, 2001). But as the amyloid cascade hypothesis alone cannot possibly solve the riddle of AD, other hypotheses including the tau hypothesis and cholinergic hypothesis have been proposed over the years.

1.2 Cholesterol and AD: Assimilated evidence suggests that brain, which accounts for ~2% of the total body weight contains the highest levels of cholesterol, i.e. ~25% of the total cholesterol synthesized in the body (Dietschy & Turley, 2004). Cholesterol in the brain is mostly derived endogenously, especially from oligodendrocytes, astrocytes and to some extent neurons, as plasma cholesterol cannot cross the blood-brain barrier (Bjorkhem & Meaney, 2004). APOE is a lipid carrier molecule which has a special relevance to nervous tissue as it was shown to coordinate the mobilization and redistribution of cholesterol during development and growth following an injury to the nervous system (Boyles et al., 1989; Mahley, 1988). APOE also plays a pivotal role in the mobilization of cholesterol and phospholipids during membrane restructuring in the central nervous system (CNS) associated with synaptic plasticity (Boyles et al., 1989; Poirier et al, 1991; Poirier et al., 1993). The inheritance of the $\epsilon 4$ allele of APOE is also a major risk factor for AD, with proven correlation between gene dose, age of onset and cognitive decline (Blacker et al., 1997; Blacker, 1997). After the age of 65, the risk of AD increases depending on the number of $\epsilon 4$ alleles present in the particular individual. Further investigation demonstrated a protective effect of the $\epsilon 2$ allele for familial and sporadic AD (Corder et al., 1994; Talbot et al., 1994). However, the mechanisms by which APOE isoforms are involved in the pathogenesis of AD are not yet elucidated. The finding that APOE is detected in the characteristic lesions associated with AD brains, i.e. extracellular senile plaques, NFTs and A β -containing blood vessels (Namba et al., 1991; Yamaguchi et al., 1991), opened new perspectives about the involvement of

APOE in AD pathogenesis. An increasing number of studies now focus on the interactions of APOE isoforms with key molecules of AD pathology. Thus, examining possible correlations between possession of the $\epsilon 4$ allele and the number, size or degree of severity of the key lesions of AD has been a common approach. In fact, with the emergence of the amyloid cascade hypothesis, a lot of interest has been directed to unraveling the association, if any, between the $\epsilon 4$ allele and A β deposition. Several investigators demonstrated that brains from $\epsilon 4$ AD patients contain significantly more amyloid plaques compared to $\epsilon 3$ patients and that plaque density correlates positively with the number of $\epsilon 4$ alleles (Beffert et al., 1999; Ishii et al., 1997; McNamara et al., 1998; Schmechel et al., 1993). APOE4 increases A β -induced neurotoxicity (Ma, Zhao, & Xia, 2009) and is more efficient than APOE3 in promoting amyloid fibril formation (Castano et al., 1995; Ma et al., 2009; Strittmatter et al., 1993).

Cholesterol has been shown to influence a number of processes involved in the generation of the neuritic plaques and NFTs (Bodovitz & Klein, 1996; Koudinov & Koudinova, 2001). Increased cholesterol levels, especially in the membrane, can induce the activity of the β -secretase pathway, leading to an increased production/accumulation of A β_{1-40} and A β_{1-42} peptides in the brain (Howland et al., 1998). Cholesterol has also been suggested to alter the conformation of A β peptide, promoting the formation of amyloid fibrils (Howland et al., 1998). It has been reported that cholesterol is capable of modulating the production of mature glycosylated APP (Galbete et al., 2000). In a transgenic mouse model, high dietary cholesterol has been shown to accelerate pathologies related to AD, including A β deposition (Refolo et al., 2000). In some reports, increased levels of midlife total cholesterol are found to be associated with a two- to threefold increased risk of developing dementia and AD later in life (Kivipelto et al., 2002). Statins are the most prescribed and effective lipid-altering drugs given their efficacy in decreasing cholesterol levels in the blood, tolerance and safety for long-time treatments (Jones, 2001). Epidemiological, *in vitro* culture and animal studies showed that statins, through the reduction of cholesterol levels and

inhibition of protein prenylation, can i) reduce the risk of developing AD and dementia by about 60% to 73% and ii) decrease the production of A β by ~50% through inhibition of APP cleavage *via* γ - and β -secretases which leads to reduced plaque formation in the brain (Fassbender et al., 2001; Gellermann et al., 2006).

1.3 Niemann Pick type C (NPC) Disease: NPC is an autosomal recessive neurodegenerative disease. The age of onset can vary from early infancy to adulthood and the clinical manifestations are heterogeneous. The infantile form of NPC is rapidly progressive and the patients usually die before two years of age of neonatal cholestasis (i.e. conjugated hyperbilirubinemia in the newborn with conjugated bilirubin levels exceeding 15% of total bilirubin levels, also known as neonatal jaundice) and/or of liver failure. NPC patients with the “classic” form of the disease get their first symptoms in early childhood before school age, with death occurring before the age of 20. Symptoms in the classic form include hepatosplenomegaly, ataxia, dystonia, seizures, vertical supranuclear gaze palsy (paralysis of down-gaze), and progressive dementia. The late onset form is a slowly progressive disease with the first symptoms occurring in adolescence or adulthood. NPC affects diverse ethnic groups. The prevalence of NPC has been estimated at approximately 1:150,000 (Vanier & Suzuki, 1998).

Accumulating evidence suggests that there are two NPC genes, i.e. *NPC1* and *NPC2*, which complement the functionalities of each other (Steinberg, Mondal, & Fensom, 1996; Vanier, 2010). In humans the defective gene is *NPC1* in 90-95% of the cases (Carstea et al., 1997) and it has been localised to chromosome 18q11.2 (Carstea et al., 1993). *NPC2* was recently identified as the protein mutated in the minor complementation group and was mapped to chromosome 14q24.3 (Naureckiene et al., 2000). Human NPC1 protein consists of 1278 amino acids and contains 13 putative transmembrane domains and 14 putative glycosylation sites (Carstea et al., 1997). NPC2 is a 151-amino acid soluble lysosomal protein with three putative N-glycosylation sites (Naureckiene et al., 2000). Both NPC proteins are ubiquitously expressed, with highest levels of

NPC1 mRNA in steroidogenic tissues (Loftus et al., 1997), and NPC2 mRNA highest in testis, kidney and liver (Naureckiene et al., 2000). NPC1 protein resides mainly in late-endosomes and lysosomes, although some co-localization has been observed with markers of the *trans*-Golgi network, recycling endosomes and the ER (Higgins, Davies, Chen, & Ioannou, 1999) as well as caveolae (Garver et al., 2000). NPC2 has a predominantly lysosomal location (Zhang et al., 2003). One of the simplest and earliest hypotheses regarding NPC1 and NPC2 interactions is that NPC1 and NPC2 somehow function in tandem to facilitate the movement of cholesterol through the endosomal/lysosomal system. Studies in mice have shown that the two proteins are likely working in the same pathway because a cross of NPC1 and NPC2 mutant mice has similar, if not identical, disease characteristics as the parental strains (Sleat et al., 2004). Also, to date, no direct interaction between NPC1 and NPC2 has been reported. An alternative hypothesis is that NPC2 functions as a bridge to enable the free cholesterol found in the internal membranes of late endosomes to be inserted into or be transferred to the limiting membrane of the organelle for subsequent transport to other parts of the cell (Chen et al., 2005). NPC1 disease does not affect plasma lipoprotein levels or lead to vascular disease (Rogaeva et al., 1998). Demyelination and formation of NFTs similar to those observed in AD brains are evident in the brain of NPC patients (Auer et al., 1995; Suzuki et al., 1995). These patients also show the deposition of diffuse A β plaques in the presence of APOE4 gene, severe loss of cerebellar Purkinje cells, and accumulation of intracellular free cholesterol in the brain (Vanier, 2010).

1.4 Glutamate and its role in AD and NPC Disease: Glutamate, the major excitatory neurotransmitter in the CNS, is involved in fast synaptic transmission, neuronal plasticity, neurite outgrowth, learning and memory and survival of neurons (Sucher et al., 1996). Although glutamate is a crucial mediator of physiological communication between neuronal cells, under certain conditions over-activation of glutamate receptors can kill neurons, and this phenomenon is known as excitotoxicity (Rothman & Olney, 1995). Injured neurons release

glutamate which leads to higher concentrations of glutamate than those required for normal neuronal functioning, resulting in regulatory system changes and cellular dysfunction. Such a phenomenon, known as excitotoxicity, has been implicated in disorders such as hypoxia, ischemia, epilepsy, AD, Parkinson's disease and Huntington disease (Lynch & Guttman, 2001; Lynch & Guttman, 2002). Serum glucose is by far the most important precursor for glutamate. After glycolysis, glucose is converted to pyruvate which enters the Krebs cycle or the tricarboxylic acid (TCA) cycle. α -Ketoglutarate is produced as an intermediate product of this cycle and is converted to glutamate in a one-step transamination reaction with the aid of the enzymes glutamate dehydrogenase and amino transferase. In presynaptic neurons the level of glutamate is maintained by the two major neuronal vesicular glutamate transporters, i.e., VGLUT1 and VGLUT2, and in the postsynaptic neurons glutamate is received by the various glutamate receptors (Danbolt, 2001). Two main subtypes of glutamate receptors have been identified on the basis of their molecular and electrophysiological properties and pharmacological antagonism (Choi, 1988; Loftus et al., 1997). The two subtypes of glutamate receptors are: (a) ionotropic receptors coupled to membrane cation channels (Na^+ , K^+ , Ca^{2+}) and (b) metabotropic receptors coupled to G proteins modulating intracellular second messengers such as inositol triphosphate, calcium or cyclic nucleotides. The ionotropic receptors themselves are ligand-gated ion channels, i.e. on binding glutamate that has been released from a neighbouring cell, charged ions such as Na^+ and Ca^{2+} can pass through a channel located in the centre of the receptor complex. This flow of ions results in depolarisation of the plasma membrane and the generation of an electrical current that is propagated down axons of the neuron to the next in line. Ionotropic receptors can be divided into following three major types based on their selective agonists: (a) N-methyl-D-aspartate (NMDA); (b) α -amino-3-hydroxy-5-methyl-4-isoxazole propionate (AMPA) and (c) kainate (KA), a natural plant product isolated from *Digenea simplex* (Choi, 1988; Cotman, Geddes, Bridges, & Monaghan, 1989; Honore, Drejer, Nielsen, Watkins, & Olverman, 1987; Parsons, Danysz, & Quack, 1998). Ionotropic glutamate receptors are integral membrane proteins that assemble as

heteromeric or homomeric receptors from subunits within their respective families. Most evidence indicates that, similar to K^+ channels, four subunits are present per receptor (Ayalon & Stern-Bach, 2001; Laube, Kuhse, & Betz, 1998; Mano & Teichberg, 1998; Safferling et al., 2001). The metabotropic glutamate receptors (mGluRs), on the other hand, contain seven putative transmembrane domains and are coupled to a variety of signal transduction pathways *via* G proteins which generate slower synaptic responses. These receptors can induce phosphoinositide hydrolysis (Sladeczek, Pin, Recasens, Bockaert, & Weiss, 1985; Sugiyama, Ito, & Hirono, 1987) or can regulate adenylate cyclase activity (Tanabe, Masu, Ishii, Shigemoto, & Nakanishi, 1992).

When excess glutamate is taken up from the synaptic cleft into glial cells by the excitatory amino acid transporters (EAATs), it is not reused directly but converted to glutamine and stored in vesicles. Subsequently, these vesicles are released from glial cells and glutamine transported back into the presynaptic neuron, converted to glutamate and stored in the vesicles by the action of VGLUTs (Pow & Robinson, 1994). This process is known as glutamate-glutamine cycle. In this cycle, glial cells release glutamine, which is then taken up into presynaptic terminals and metabolized into glutamate by the enzyme glutaminase. The glutamate synthesized in the presynaptic terminal is packaged into synaptic vesicles by VGLUT. Once the vesicle is released, excess glutamate is removed from the synaptic cleft by EAATs. This allows synaptic terminals and glial cells to work together in order to maintain a proper supply of glutamate (Danbolt, 2001).

The most significant changes of the glutamatergic system in AD brains include: (1) decrease in glutamate content in cortex and hippocampus; (2) decrease in Na^+ -dependent glutamate uptake in cortex and hippocampus; (3) decrease in GluRs in hippocampus, frontotemporal cortex and nucleus basalis of Meynert; (4) decrease in AMPA GluR2/3 and GluR1 subunits in the entorhinal cortex; and (5) decrease in sensitivity and number of strychnine-insensitive glycine sites in the cortex

(Greenamyre & Young, 1989; Muller et al., 1995; Steele et al., 1989). A β peptide increases the vulnerability of cultured neurons to glutamate-induced excitotoxic damage and alters glutamate uptake by astrocytes due to a failure in energy metabolism (Parpura-Gill et al., 1997). The activity of the astrocytic glutamine synthetase (GS) is decreased in AD brains, and it appears that A β peptide negatively influences GS activity (Butterfield et al., 1997). In AD brains, phosphorylated tau accumulates in PHFs, which form NFTs in affected neurons. Glutamate and aspartate can induce PHF formation in cultured human neurons similar to those seen in AD brains (De Boni & McLachlan, 1985). Pyramidal neurons of the neocortex along with those of the entorhinal cortex and hippocampal CA1 region are degenerated in AD, whereas the remaining neurons are subject to NFT formation (Braak & Braak, 1991; Morrison & Hof, 1997a; Pearson et al., 1985). The clinical significance of these changes is highlighted by the observation that alteration in different glutamate receptors and/or glutamate levels correlate with the degree of dementia in AD patients (Francis et al., 1993). Furthermore, glutamate-immunopositive neurons have been shown to be reduced in number and subject to tangle formation in AD brains (Kowall & Beal, 1991). There was also a reduction in the vesicular glutamate transporter VGLUT1 in the parietal but not in the temporal cortex of the mutant APP transgenic mouse brains (Kirvell et al., 2006). Unlike AD pathology, neurotransmitter studies in NPC disease are very limited. One proteomic study reports a decrease in the glial glutamatergic transporters like EAAT1 in NPC1-knockout (ko) mice. It was observed that EAAT1 levels were decreased in the CA1, CA3 and dentate gyrus of 8 week old NPC1-ko mice compared to age-matched controls (Byun et al., 2006). Functional glutamate uptake and GLAST protein expression are reduced in *Gfa2-SCA7* NPC1-ko mice - a mouse model of cerebellar ataxia 7. This decrease in GLAST expression and glutamate uptake is associated with Purkinje cell degeneration (Custer et al., 2006).

1.5 GABA and its role in AD and NPC Disease: GABA was first identified in the mammalian brain over half a century ago during the 1950s (Awapara et al.,

1950), and strong evidence accumulated over the years suggests that GABA acts mostly as an inhibitory neurotransmitter in both vertebrate and invertebrate nervous systems (Roberts & Frankel, 1950; Roberts & Difiglia, 1988a). In the mammalian brain, GABA is synthesized primarily from glutamate that is catalysed by two glutamic acid decarboxylase (GAD) enzymes, GAD65 and GAD67. GABA is loaded into synaptic vesicles by a vesicular neurotransmitter transporter (VGAT) and is liberated from nerve terminals by calcium-dependent exocytosis. GABA can be released either vesicularly or non-vesicularly by reverse transport mechanisms. The effects of GABA can be mediated by the activation of either ionotropic or metabotropic GABA receptors. GABA receptors are located at both pre- and postsynaptic sites. GABA_A receptors are the ionotropic receptors which are members of the ligand-gated ion channel family of receptors. For this class of receptors, ligand binding is followed by a conformational change in the channel protein that allows a net inward or outward flow of ions through the membrane-spanning pore of the channel, depending on the electrochemical gradient of the particular permeant ion. GABA_A receptors carry primarily chloride (Cl⁻) ions; however, other anions, such as bicarbonate (HCO₃⁻), can also permeate the channel pore, although less efficiently (Bormann, 1988; Kaila, 1994). Chloride-dependent GABA_A-receptor-mediated synaptic inhibition can occur either pre- or post-synaptically. GABA_A receptors are believed to be heteropentameric proteins that are constructed from 19 different subunits derived from several related genes or gene families (Macdonald & Olsen, 1994; Cossette et. al., 2012). A related ionotropic GABA receptor, sometimes termed the GABA_C receptor, has also been identified. This receptor is a chloride-selective ion channel, but is insensitive to the GABA_A receptor antagonist bicuculline (Bormann & Feigenspan, 1995). GABA_B receptors are metabotropic receptors that cause presynaptic inhibition by suppressing calcium influx and reducing transmitter release, and achieve postsynaptic inhibition by activating potassium currents that hyperpolarize the cell (Bormann, 1988; Hannan et. al., 2012). GABA signals are terminated by reuptake of the neurotransmitter into nerve terminals and/or into surrounding glial cells by a class of plasma-membrane

GABA transporters (GATs) (Cherubini & Conti, 2001). GABA is metabolized by a transamination reaction that is catalysed by GABA transaminase (GABA-T) (Roberts & Difiglia, 1988b). In studies with AD patients, decreases of GABA levels and the GABA/glutamate ratio and also GABA uptake sites have been reported in selected brain regions (Garcia-Alloza et al., 2006). GAD activity was found to be unaltered in the AD brain compared to age-matched control brains (Reinikainen et al., 1988). Radioligand binding studies demonstrate mild reductions in GABA_A or benzodiazepine binding sites in the AD brain (Greenamyre et al., 1987; Vogt, Crino, & Volicer, 1991). In case of NPC disease, an increase in the glial GABA transporter GAT3 and GABA levels were evident from a proteomics study in NPC1-ko mice. It was observed that there was an increase in GAT3 levels in CA1 and CA3 regions of hippocampus in 4 week old NPC1-ko mice but not in the dentate gyrus compared to age-matched controls. In 8 week old NPC1-ko mice, there was a significant increase in the levels of GAT3 in CA1, CA3 and dentate gyrus of hippocampus as well as a reduction in GAD67 levels in all these regions of hippocampus compared to age-matched controls (Byun et al., 2006).

1.6 Hypothesis: To study the possible role of disturbances in cholesterol metabolism on AD pathology, our lab has recently developed a novel transgenic mouse line that over-expresses mutant human APP in the absence of functional Npc1 protein by crossing the TgCRND8 APP-transgenic line (Chishti et al., 2001) with heterozygous NPC1-ko mice (Maulik et al., 2012). These mice have an accelerated AD and NPC pathologies and are termed ANPC mice. The ANPC mice are relatively smaller in size and have a significantly lower body weight and slower growth rate compared to other littermates. These mice have an average life expectancy of about 70 days and they exhibit intracellular cholesterol accumulation along with exacerbated glial pathology with increased proliferation and activation of astrocytes and microglia. These mice also show severe demyelination and loss of cerebellar Purkinje neurons at 7 weeks of age, whereas in 10 week old mice A β plaques are observed in the cortex and the hippocampus.

The double-mutant ANPC mice also display cognitive and motor deficits as observed in object-recognition and rotarod behavioural tests. Given the importance of glutamate and GABA in normal brain functioning and the fact that these two neurotransmitter systems are affected in both AD and NPC diseases, we hypothesize that the glutamatergic and GABAergic neurotransmitter systems will be impaired in the brains of our bigenic ANPC mice brain compared to other littermates.

2. Materials and Methods

2.1 Materials: DNA and RNA isolation kits were from Qiagen Inc. (Mississauga, ON, Canada), whereas the enhanced chemiluminescence (ECL) kit and bicinchoninic acid (BCA) protein assay kit were obtained from Pierce Fisher Scientific (Montreal, QC). Polyclonal anti-GAD65, monoclonal anti-GAD67 and anti-NeuN (Neuronal marker) antisera were purchased from Millipore Int. (Temecula, CA), whereas polyclonal anti-VGLUT1 and anti-VGLUT2 were obtained from Synaptic Systems (Goettingen, Germany). Anti- β -actin and anti-calbindin D-28K antisera were obtained from Sigma-Aldrich (Oakville, ON). All horseradish peroxidase (HRP)-conjugated secondary antibodies were purchased from Santa Cruz Biotechnology (Paso Robles, CA), whereas fluorescent secondary antisera conjugated to either Texas Red or Fluorescein isothiocyanate (FITC) Alexa Fluor-488 were from Jackson ImmunoResearch (West Grove, PA) and Molecular Probes/Invitrogen (Burlington, ON), respectively. SDS PAGE gels (7-17%) were made in the laboratory using a gradient mixer. Individual amino acid standards and *o*-phthaldialdehyde (OPA) were obtained from Sigma Chemical Co. (St. Louis, MO). *N*-Isobutyryl-L-cysteine was purchased from Novabiochem (La Jolla, CA). All solvents were of HPLC grade and water was distilled and purified by reverse osmosis before use. All other reagents were from Sigma-Aldrich (Oakville, ON) or Fisher Scientific (Montreal, QC).

2.2 Animals: Mutant human APP transgenic mice maintained on a C3H/C57BL6 background were obtained from Dr. David Westaway's group (Centre for Prions and Protein Folding Diseases, University of Alberta) and heterozygous *Npc1* gene knock-out (*Npc1*^{-/-}) mice maintained on BALB/c strain background were obtained from Dr. Jean E. Vance (Department of Medicine, University of Alberta). The APP transgenic mice carry the APP695 isoform with Swedish (K670M/N671L) and Indiana (V717F) mutations. These two parental mice lines were crossed to generate APP^{+/+}*Npc1*^{+/-} and APP^{-/-}*Npc1*^{+/-} F1 progeny on a mixed C3H/C57BL6/BALB/c strain background which were subsequently inter-crossed

to produce all five genotype combinations (WT, APP-Tg, Dhet, NPC1-ko and ANPC) (Table 1) used in this study. All animals were bred and housed in our own colony with a maximum of 5 animals per cage maintained on a 12 h light/dark cycle and access to food and water *ad libitum*. The maintenance of the colony and experiments included in the thesis were performed in accordance with University of Alberta and Canadian Council of Animal Care guidelines.

2.3 DNA analysis: Transgenic/ko mice were genotyped by polymerase chain reaction (PCR) of tail DNA obtained at postnatal day 21. In brief, the tail from each mouse was first digested overnight at 55°C with proteinase K and DNA was isolated using DNeasy blood and tissue kit and stored at 4°C until use. For genotyping two sets of primers were used: one for amplifying the human APP transgene (5'-TGTCCAAGATGCAGCAGAACGGCTACGAAA A-3' and 5'-AGAAATGAAGAAACGCCAAGCGCCGTGACT-3') and the second to amplify mouse NPC1 gene (5'-GGTGCTGGACAGCCAAGTA-3' and 5'-GATGGTCTGTTCTCCC ATG-3'). PCRs were carried out in 25 µl reaction volume for 35 cycles with Top Taq DNA polymerase (Qiagen Inc., Canada) and 1 µmol of each primer (Integrated DNA Technologies, IDT, University of Alberta). Amplification of NPC1 locus with primers flanking the insertion locus revealed a size alteration of the knock-out gene product. The PCR products are run into 1.5% agarose gels to ascertain their molecular sizes and subsequent genotyping. Molecular size of wild-type (WT) product was observed to be 1056 bp and that of NPC1 knock-out (NPC1-ko) allele to be of 1200 bp. Similarly, amplification of APP transgene was detected by the presence of a single band of ~1000 bp while the absence of a similar sized band indicated the WT genotype. Table-1 shows mice genotypes and their abbreviations used in the present study.

Table 1.

<i>Npc1</i> genotype	<i>APP</i> genotype	Line of Mice
+/+	-/-	WT
+/+	+/-	APP-Tg
+/-	-/-	<i>Npc1</i> -Het
+/-	+/-	Dhet
-/-	-/-	NPC1-ko
-/-	+/-	ANPC

2.4 Tissue Collection: The ANPC mice and their age-matched siblings (WT, APP-Tg, Dhet and NPC1-ko) were collected at 4, 7 and 10 weeks of age. Mice were decapitated by cervical dislocation and brains were removed and bisected on ice. One half of the brain was fixed in 4% paraformaldehyde for 24 h at 4°C, washed with phosphate-buffered saline (PBS, pH 7.2) and then stored in 30% sucrose until further processing for histological/ immunohistochemical staining. The other half of the brain was dissected into cerebellum, hippocampus, striatum and frontal cortex, which were then snap-frozen in dry ice and stored at -80°C for biochemical analysis.

2.5 Western Blotting: Selected brain regions (frontal cortex and cerebellum) from five different genotypes (WT, APP-Tg, Dhet, NPC1-ko and ANPC, n=4/genotype) were lysed in modified RIPA buffer [20 mmol/L Tris-HCl (pH 8), 150 mmol/L NaCl, 0.1% sodium dodecyl sulfate, 1 mmol/L ethylenediamine-tetraacetic acid, 1% Igepal CA-630, 50 mmol/L NaF, 1 mmol/L NaVO₃, 10 µg/ml leupeptin, and 10 µg/ml aprotinin] and then centrifuged at 10,000 rpm for 10 min. The supernatants were collected and protein content was measured by the BSA assay. Equal amounts of denatured protein were loaded and separated on a 7-17% SDS-PAGE and then transferred to nitrocellulose membranes. The

membranes were blocked in 5% non-fat milk in TBST [10 mM Tris-HCl (pH 8.0), 150 mM NaCl, and 0.2% Tween-20] and then incubated overnight at 4°C with anti-GAD67 (1:5000), anti-GAD65 (1:5000), anti-VGLUT1 (1:7500) and anti-VGLUT2 (1:7500). After incubation, the blots were washed with TBST for 30 min and incubated with appropriate horseradish peroxidase (HRP)-conjugated secondary antibodies (1:5000) for 1h at room temperature. The blots were finally washed with TBST for 30 min and signals were visualized with an ECL detection system. Blots were subsequently reprobed with anti- β -actin (1:5000) and quantified using a MCID image analyzer as described earlier (Kodam et al., 2010).

2.6 Immunohistochemistry: Paraformaldehyde-fixed hemibrains from five different genotypes (WT, APP-Tg, Dhet, NPC1-ko and ANPC, n=4/genotype) were sectioned at 20 μ m using a cryostat and then processed for histological/immunohistochemical staining using a free-floating procedure. In brief, frontal cortex and cerebellar sections from WT, APP-Tg, Dhet, NPC1-ko and ANPC mice of two different age groups (4 and 10 weeks) were washed in PBS in 3 changes of 10 mins each and then treated with boiling citrate buffer (pH 6.0) for 20 mins. For the frontal cortex, sections after treatment with citrate buffer were incubated overnight at room temperature with either anti-GAD67 (1:200), anti-GAD65 (1:5000), anti-VGLUT1 (1:1000) and anti-VGLUT2 (1:1000) antisera along with neuronal marker anti-NeuN (1:25,000) for double fluorescence staining. For the cerebellum, sections after the treatment with citrate buffer were incubated overnight with anti-VGLUT1 (1:1000) or anti-VGLUT2 (1:1000) antisera along with anti-calbindin D-28K (1:1000) antisera for double fluorescence staining. The sections were then washed with PBS, incubated with appropriate Alexa Fluor-488 (1:500), Texas red (1:200) or FITC (1:200) conjugated secondary antibodies for 2h at room temperature, washed with PBS for 30 mins and finally mounted with VectaShield mounting medium. Immunostained sections were examined and photographed using a Zeiss Axioskop-2 microscope.

2.7 High Performance Liquid Chromatography (HPLC)

2.7.1 Apparatus: HPLC was performed using a Waters Alliance 2690XE instrument equipped with an autosampler, thermally controlled sample and column compartments, and a Waters 474 programmable fluorescence detector (Waters Corporation, Milford MA) as described earlier (Kabogo et al., 2010). Data were acquired and processed using the Empower Pro software package from Waters. Separation was carried out on a Symmetry C₁₈ column (4.6 mm × 150 mm, 3.5 μm) coupled with a guard column containing the same stationary phase (3.9 mm × 20 mm, 5 μm), both from Waters as described in detail earlier (Grant et al., 2006).

2.7.2 Chromatographic conditions: The sample and column compartments were maintained at 4° and 30°C, respectively, for all analyses. The flow rate was constant at 0.5 mL/min and run time was 60 min. Solvent A comprised 1700 mL 0.04 M sodium phosphate and 1.42 gm disodium phosphate and 300 mL methanol, adjusted to pH 6.2. Solvent B comprised 1340 mL 0.04 M sodium phosphate, 1110 mL methanol and 60 mL tetrahydrofuran adjusted to pH 6.2. This particular composition of solvent B has been used in our lab previously when we were analyzing amino acids after derivatization with OPA in combination with mercaptoethanol (Grant et al., 2006). Mobile phases were filtered through a 0.2 μm filter prior to use. The amino acids of interest were separated by a concave gradient (Curve 8 in Waters Empower Pro software) from 10% to 90% B in 45 min. The solvent mix was returned to initial conditions by 45 min using a concave gradient (Curve 9 in Waters Empower Pro software) and maintained at that composition for 15 min prior to the next injection. Many gradient profiles were tested and this particular concave gradient was found to give the best separation.

2.7.3 Derivatization procedures: Derivatizing reagent solutions were prepared by dissolving 2 mg OPA and 3 mg Isobutyryl chloride (IBCL) in 150 μl methanol followed by the addition of 1350 μl 0.1 M sodium borate buffer (pH 10). The

reagent solutions were prepared freshly every second day and stored at 4°C when not in use. Automated pre-column derivatization was carried out by drawing up a 5 µL aliquot of sample, standard, or blank solution and 5 µL of derivatizing reagent solution, and holding in the injection loop 5 min prior to injection.

2.7.4 Standard solutions: Stock solutions of L-glutamate (L-Glu), L-glutamine (Gln), L-serine (L-Ser), D-serine (D-Ser), L-aspartic acid (Asp), L-arginine (Arg), glycine (Gly), L-alanine (Ala) and GABA were prepared in 40% (v/v) methanol in RIPA buffer at a concentration of 1.0 mg/mL. An intermediate standard mixture was prepared by combining 40 µL of L-Glu, 20 µL L-Gln stock solutions, 10 µL each of L-Ala and GABA stock solutions and 5 µL each of L-Ser, D-Ser, and Gly stock solutions with 905 µL 40% (v/v) methanol. For calibration using a 7-point standard curve, this intermediate standard was diluted to 0.75, 0.5, 0.25, 0.1, 0.025, and 0.01 times its original strength.

2.7.5 Sample Preparation: Frontal cortical and cerebellar tissues from 4, 7 and 10 week old mice from different genotypes (WT, APP-Tg, Dhet, NPC1-ko and ANPC, n=4/genotypes) were homogenized separately in 5 vols of RIPA buffer. A portion of the homogenate from each of these samples was diluted in 450 µL of ice-cold methanol, vortexed well and kept on ice for 10 mins (x60 dilution). Subsequently, the homogenate was centrifuged at 12,000 rpm for 5 mins and the supernatant was again centrifuged under similar conditions. A portion (100 µL) of supernatant from the second spin was then transferred to a HPLC vial for the detection of possible changes in glutamate and GABA levels in the ANPC mice compared to other genotypes as described earlier (Amritraj et al., 2011). The remainder of the sample was used for protein estimation by BCA protein assay.

2.8 Data Analysis: Data are expressed as mean ± SEM. One-way ANOVA followed by Newman-Keuls post-hoc analysis was applied to study the relationship between groups. $p < 0.05$ was considered to be significant.

3. Results

3.1 Determination of glutamate and GABA levels in the frontal cortex and cerebellum of ANPC mice:

We used HPLC to determine glutamate and GABA content in both the frontal cortex and the cerebellum of ANPC mice compared to age-matched WT, APP-Tg, Dhet and NPC1-ko mice. To observe the changes we used two age groups: 4 week and 10 week old mice. The values obtained from the HPLC showed the amount of amino acid per mg of the tissue which were subsequently converted into amounts of amino acid per mg of protein. In the frontal cortex, the endogenous levels of glutamate was found to be unaltered at 4 and 10 week old ANPC mice compared to the age-matched WT, APP-Tg, Dhet and NPC1-ko mice. In the cerebellum, the levels of glutamate were also found to be unaltered at 4 and 10 weeks of age in ANPC mice compared to other lines of mice (Fig. 1). In case of GABA, the same trend as observed with glutamate was evident in both the frontal cortex and cerebellum of ANPC mice. At 4 and 10 weeks of age the endogenous levels of GABA in the frontal cortex were found to be unaltered in the ANPC mice compared to the age-matched WT, APP-Tg, Dhet and NPC1-ko mice. Similarly, there were no significant alterations in the cerebellar GABA levels either in 4 or 10 week old ANPC mice compared to the age-matched WT, APP-Tg, Dhet and NPC1-ko mice (Fig. 2).

3.2 Determination of the levels of glutamatergic and GABAergic markers in the frontal cortex and cerebellum of ANPC mice:

To determine the possible alterations of the glutamatergic and GABAergic markers in the frontal cortex and cerebellum of WT, APP-Tg, Dhet, NPC1-ko and ANPC mice, the steady state protein levels were measured by western blotting. In this case, three distinct time points: i.e. 4, 7 and 10 weeks, were used to evaluate the changes in the protein expression levels with the progression of the disease pathology. The glutamatergic markers used in the study were VGLUT1 and VGLUT2 and the GABAergic markers were GAD65 and GAD67.

VGLUT1: The VGLUT1 antibody detected a 62kDa band in the mouse brain, as reported in earlier studies (Zhou et al., 2007). Our western blot data obtained with the antibody revealed a significant age-dependant decrease in VGLUT1 levels in the frontal cortex of ANPC mice compared to the WT, APP-Tg, Dhet and NPC1-ko mice. At 4 weeks, the ANPC mice showed significant decreases with respect to the WT, APP-Tg and Dhet mice. At 7 weeks of age the ANPC mice showed a marked decrease ($p<0.01$) in VGLUT1 levels compared to WT, APP-Tg, and Dhet mice. However, the NPC1-ko mice did not show any significant alterations with respect to the WT, APP-Tg, Dhet or ANPC mice either at 4 or 7 weeks of age. Interestingly, at 10 weeks of age, the ANPC mice showed a marked decrease in VGLUT1 levels compared to all other lines i.e. WT, APP-Tg, Dhet and NPC1-ko mice ($p<0.01$) (Fig. 3). In contrast to the frontal cortex, VGLUT1 levels in the cerebellum of ANPC mice showed a decrease with the progression of the disease. At 4 weeks of age, the ANPC mice did not show any significant change in the steady-state VGLUT1 levels with respect to age-matched other lines of mice. At 7 weeks, however, ANPC mice not only showed a significant ($p<0.05$) reduction in VGLUT1 levels with respect to WT, APP-Tg and Dhet mice, but the NPC1-ko mice also exhibited a marked reduction in VGLUT1 levels compared to the WT mice. A similar profile was obtained at 10 weeks in cerebellum where both ANPC and NPC1-ko mice showed significant ($p<0.01$) reductions in the VGLUT1 levels compared to WT, APP-Tg and Dhet mice (Fig. 4).

VGLUT2: The VGLUT2 antibody detected a 65kDa band in the mouse brain, as reported in earlier studies (Zhou et al., 2007). The VGLUT2 did not display any marked alteration in either the frontal cortex or the cerebellum at any time point. In the frontal cortex, our data showed no significant alteration in the steady state protein levels either at 4, 7 or 10 weeks of age compared to WT, APP-Tg, Dhet and NPC1-ko littermate mice (Fig. 5). Similarly, in the cerebellum the VGLUT2 level was found to be unaltered in both the ANPC and NPC1-ko mice compared to the WT, APP-Tg, and Dhet mice at 4, 7, and 10 weeks time points.

Interestingly, VGLUT2 showed a trend of increase in 10 week old ANPC mice compared to the WT mice, but it did not reach significance (Fig. 6).

GAD65: The GAD65 antibody detected a 65kDa band in the mouse brain, as reported in earlier studies (Zander et al., 2010). The GABAergic marker, GAD65, did not show any significant change either in the frontal cortex or cerebellum of ANPC mice at any age group compared to WT, APP-Tg, Dhet and NPC1-ko mice. In the frontal cortex, GAD65 levels remained unchanged in the ANPC mice compared to the other lines of mice at 4, 7 and 10 weeks of age (Fig. 7). In the cerebellum too, GAD65 remained unaltered at 4, 7 and 10 weeks compared to the other lines of mice (Fig. 8). Similarly, the level of GAD65 was also unaltered in both the frontal cortex and cerebellum of the NPC1-ko mice at all age groups studied compared to WT, APP-Tg and Dhet lines of mice.

GAD67: The GAD67 antibody detected a 67kDa band in the mouse brain, as reported in earlier studies (Sakai, 2011). In the case of GAD67, changes in protein expression levels were observed in the cerebellum but not in the frontal cortex of the ANPC mice compared to the other lines of mice. In the frontal cortex, the ANPC mice did not show any significant changes in GAD67 levels either at 4, 7 or 10 weeks of age with respect to WT, APP-Tg, Dhet and NPC1-ko mice (Fig. 9). However, in the cerebellum, there was a decrease in the steady state GAD67 levels with the progression of disease pathology. At 4 weeks of age ANPC mice did not reveal any significant alterations in GAD67 levels compared to age-matched WT, APP-TG, Dhet and NPC1-ko mice. However, at 7 weeks of age the ANPC mice showed a significant ($p < 0.05$) decrease in GAD67 levels compared to age-matched WT, APP-Tg, and Dhet lines. At 10 weeks of age the ANPC mice showed a further decrease in the levels of GAD67 with respect to the WT, APP-Tg, and Dhet mice. Both at 7 and 10 weeks of age, GAD67 levels were also found to be significantly ($p < 0.01$) decreased in the NPC1-ko mice compared to the WT, APP-Tg and Dhet mouse lines, but there was no marked alteration between ANPC and NPC1-ko lines at any time point (Fig. 10).

3.3 Determination of the changes in the distribution profile of glutamatergic and GABAergic markers in ANPC mice: To observe the changes in the distribution profile of the glutamatergic and GABAergic markers in the ANPC mice, immunohistochemical analysis was performed in five different lines of mice. Free floating sections from frontal cortex region were stained with VGLUT1, VGLUT2, GAD67 and GAD65 antibodies along with the neuronal marker NeuN to show the co-localization of these proteins with neurons. As for the cerebellum, double staining was performed with either VGLUT1 or VGLUT2 along with Calbindin D-28k which labels specifically the GABAergic Purkinje cells. Immunohistochemical staining was performed at two time points, i.e. 4 and 10 weeks, to ascertain possible alterations in the distribution profile of these markers.

Frontal cortex: Both glutamatergic markers VGLUT1 and VGLUT2 showed punctate immunostaining representing the glutamatergic boutons/nerve terminals all through the frontal cortex. At 4 weeks, VGLUT1 immunoreactive puncta were evident in all areas of the frontal cortex in the WT, APP-Tg, Dhet and NPC1-ko mice, whereas the staining appeared to be less intense in the ANPC mice (Fig. 11). A similar profile was observed at 10 weeks, where the VGLUT1 immunostaining in ANPC appeared to be lower than that observed in the WT, APP-Tg, NPC1-ko and Dhet mice (Fig 12). At both time points, there were no detectable alterations in the NeuN immunostaining, suggesting that there is possibly no loss of neurons in the frontal cortex of the ANPC mice compared to other lines of mice. In the case of VGLUT2, the immunostaining profile appeared to be similar to that observed with VGLUT1. At 4 weeks the intensity of immunostaining in the cortex of ANPC mice appeared to be less than that evident in WT, APP-Tg, Dhet and NPC1-ko mice (Fig. 13). At 10 weeks of age, a similar pattern was observed in the ANPC mice compared to other lines of mice (Fig. 14). With regard to the GABAergic markers, GAD67 is a cytosolic protein which identifies GABAergic cell bodies and some boutons, whereas GAD65 is a membrane protein that labels the membrane of the neurons. The frontal cortex of

ANPC mice did not show any change in the distribution or intensity in GAD67 staining at either 4 weeks or 10 weeks of age compared to the WT, APP-Tg, Dhet and NPC1-ko mice (Fig. 15 and 16). At both time points, co-localization of the GAD67-positive GABAergic neurons with immunoreactive NeuN was evident. In case of GAD65, a similar profile was apparent in the ANPC mice compared to the other lines of mice at both 4 and 10 weeks of age (Fig 17 and 18). It appears that, unlike the glutamatergic markers, neither of the GABAergic markers showed any marked alteration in the frontal cortex of the ANPC mice compared to the other lines of mice.

Cerebellum: In the cerebellum, double staining was performed with either of the glutamatergic markers, i.e. VGLUT1 and VGLUT2, along with the GABAergic marker calbindin D-28k. Both glutamatergic markers, which exhibited a similar pattern of staining, displayed dense puncta in the granular cell layer followed by VGLUT1/2 immunoreactive puncta surrounding the Purkinje neurons under normal conditions. A number of distinct VGLUT1 and VGLUT2 immunoreactive boutons were observed in the molecular layer of normal control cerebellum. In the NPC1-ko and the ANPC mice a marked loss of Purkinje neurons was evident from 7 weeks onwards (Maulik et al., 2012). At 10 weeks of age, the Purkinje cell layer has almost completely disappeared in the ANPC and NPC1-ko mouse brains. Calbindin D-28k, staining which specifically labels the Purkinje neurons in the cerebellum, showed an intact layer, without any loss of cells, at 4 weeks of age in all lines of mice. But at 10 weeks of age calbindin D-28k staining did not reveal the presence of any Purkinje neurons either in the ANPC or NPC1-ko mouse brains. These results suggest a loss of GABAergic neurons in 10 week old ANPC and NPC1-ko mice. In the case of VGLUT1 immunostaining, no marked alteration was evident in 4 week old ANPC mice compared to WT, APP-Tg, Dhet and NPC1-ko mice. But at 10 weeks of age, due to the absence of the Purkinje neurons in both the ANPC and NPC1-ko mice, VGLUT1 immunostaining was not apparent in the Purkinje cell layer and the amount of visible boutons in the molecular layer appeared to be decreased. Interestingly, in the granular cell layer

a number of VGLUT1 puncta were still present in both ANPC and NPC1-ko mice (Fig. 19). The VGLUT2 immunoreactivity showed a similar profile as observed with VGLUT1. There was no visible alteration in the VGLUT2 immunostaining in 4 weeks old ANPC and NPC1-ko mice compared to other lines of mice. At 10 weeks of age there seemed to be a decrease in the intensity of the VGLUT2 immunostaining in the Purkinje and molecular layers of the NPC1-ko and ANPC mice compared to the WT, APP-Tg and Dhet mice (Fig. 20).

FIGURES:

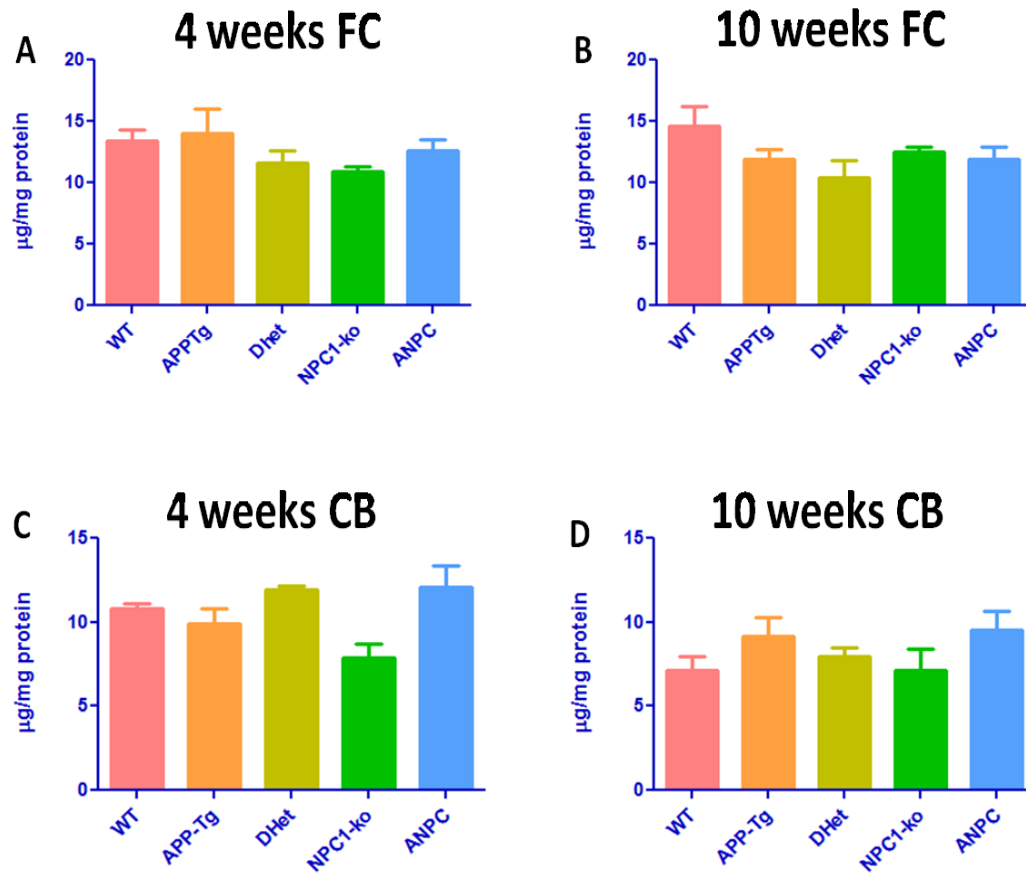


Fig 1: Quantitative analysis of glutamate levels in the frontal cortex (FC) (A and B) and cerebellum (CB) (C and D) of ANPC mice compared to the other lines of mice at 4 and 10 weeks of age. No significant alteration was evident in any brain region. Data are expressed as mean \pm SEM (n=4).

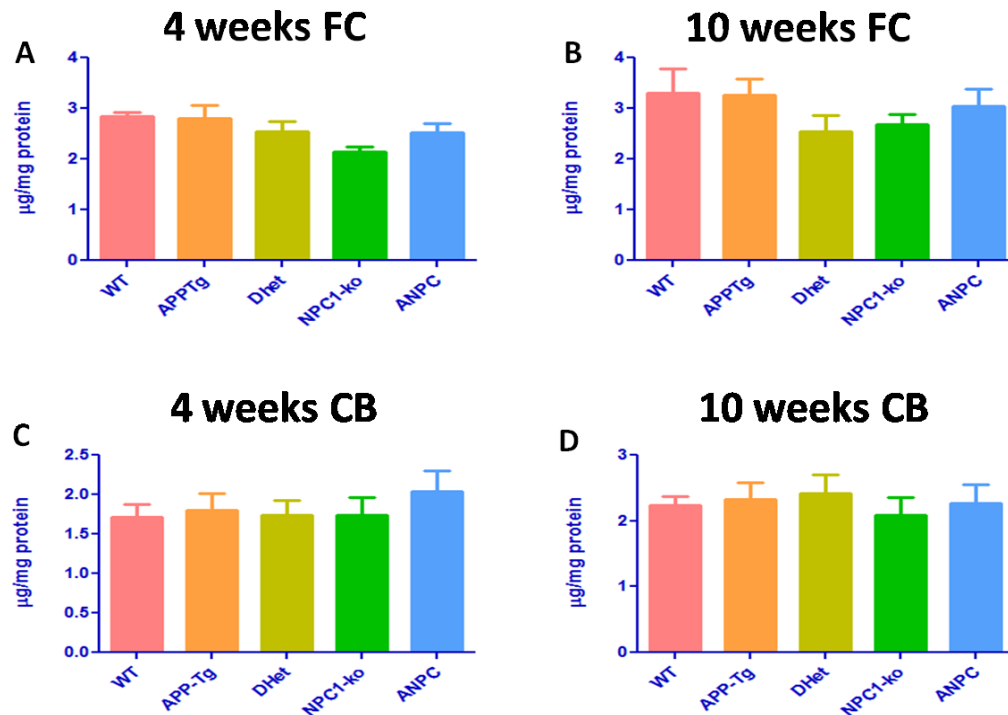


Fig 2: Quantitative analysis of GABA levels in the frontal cortex (FC) (A and B) and cerebellum (CB) (C and D) of ANPC mice compared to the other lines of mice at 4 and 10 weeks of age. No significant alteration was evident in any brain region. Data are expressed as mean \pm SEM (n=4).

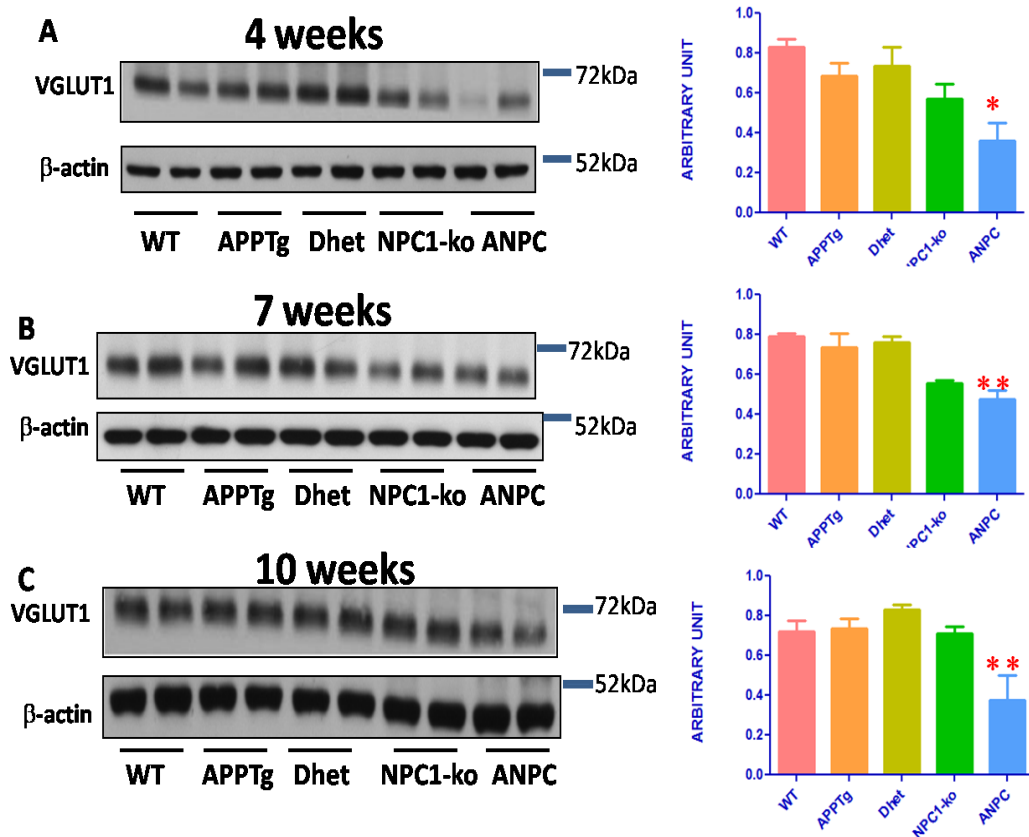


Fig 3: Western blots and corresponding histograms showing the levels of VGLUT1 in the frontal cortex of the ANPC mice compared to other littermates at 4 (A), 7 (B) and 10 (C) weeks of age. Note the significant decrease in the level of VGLUT1 in the ANPC mice at all the time points with respect to the WT, APP-Tg, Dhet and NPC1-ko mice. Data are expressed as mean \pm SEM and * $p < 0.05$, ** $p < 0.01$ (n=4).

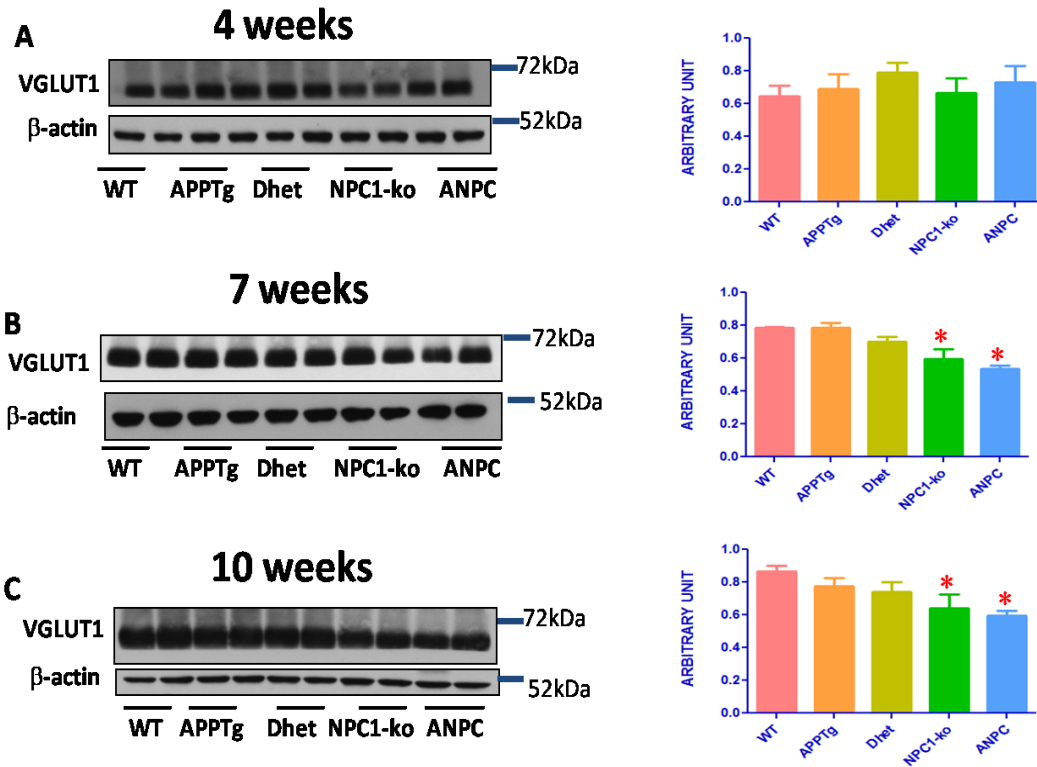


Fig 4: Western blots and corresponding histograms showing the levels of VGLUT1 in the cerebellum of the ANPC mice compared to other littermates at 4 (A), 7 (B) and 10 (C) weeks of age. Note the significant decrease in the level of VGLUT1 in the ANPC mice at 7 and 10 weeks of age with respect to the WT, APP-Tg and Dhet mice. NPC1-ko mice also showed a significant decrease with respect to the WT mice. Data are expressed as mean \pm SEM and * $p < 0.05$ (n=4).

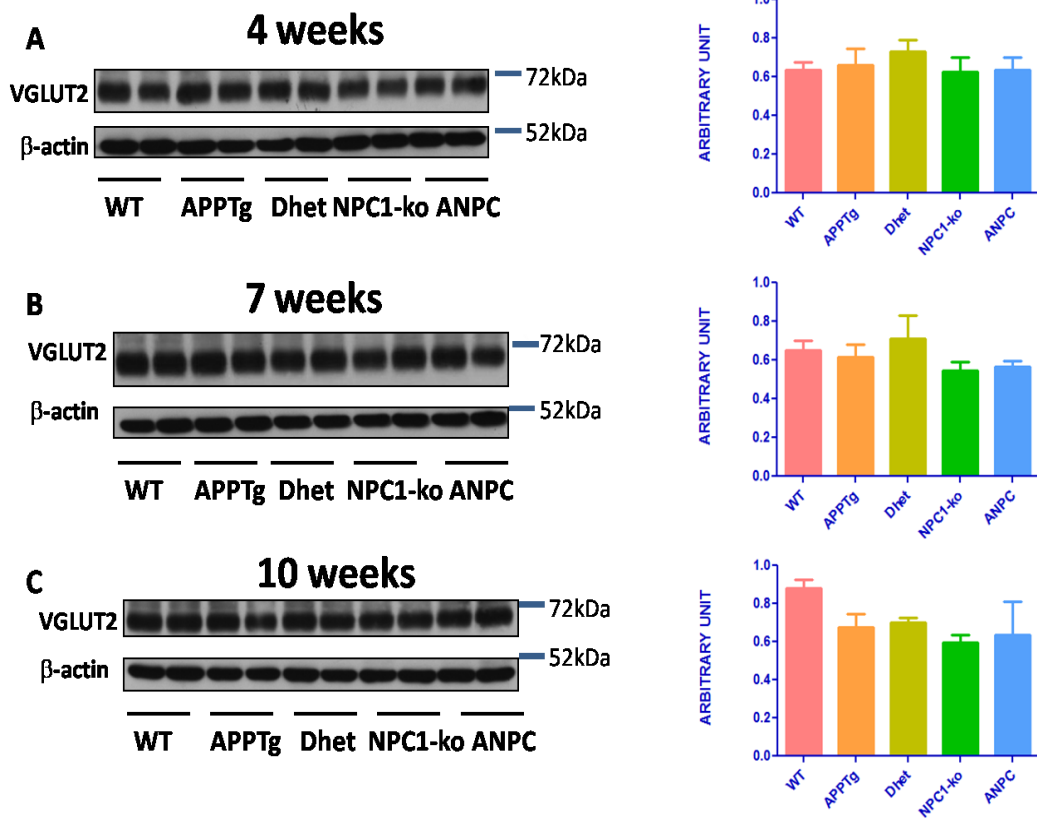


Fig 5: Western blots and corresponding histograms showing the levels of VGLUT2 in the frontal cortex of the ANPC mice compared to other littermates at 4 (A), 7 (B) and 10 (C) weeks of age. Note the absence of significant alterations in the level of VGLUT2 in the ANPC mice at any the time points with respect to the WT, APP-Tg, Dhet and NPC1-ko mice. Data are expressed as mean \pm SEM (n=4).

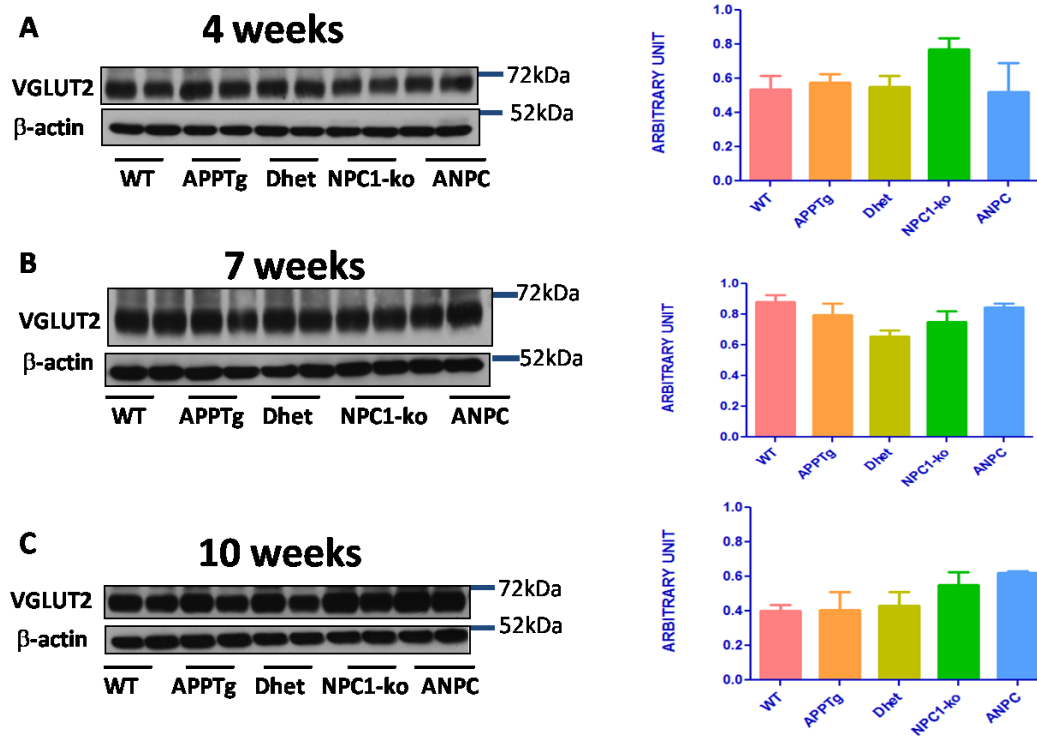


Fig 6: Western blots and corresponding histograms showing the levels of VGLUT2 in the cerebellum of the ANPC mice compared to other littermates at 4 (A), 7 (B) and 10 (C) weeks of age. Note the absence of significant alterations in the level of VGLUT2 in the ANPC mice at any the time points with respect to the WT, APP-Tg, Dhet and NPC1-ko mice. Data are expressed as mean \pm SEM (n=4).

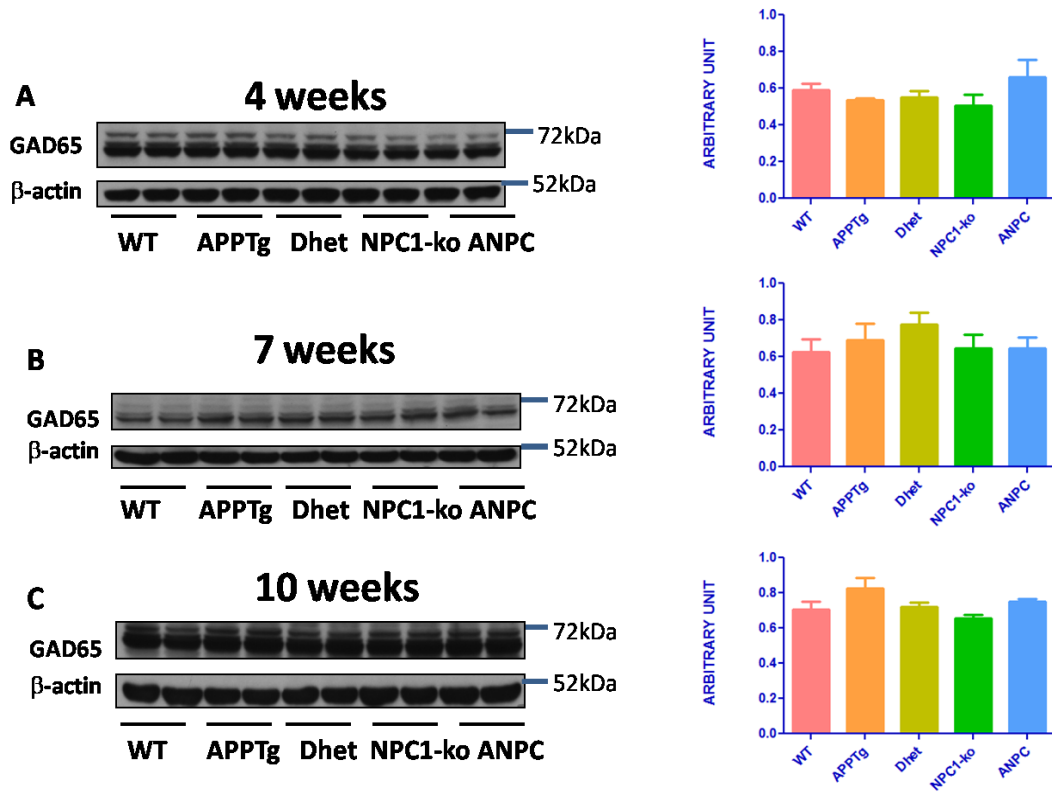


Fig 7: Western blots and corresponding histograms showing the levels of GAD65 in the frontal cortex of the ANPC mice compared to other littermates at 4 (A), 7 (B) and 10 (C) weeks of age. Note that quantitative analysis showed no alterations in the level of GAD65 in the ANPC mice at any the time points with respect to the WT, APP-Tg, Dhet and NPC1-ko mice. Data are expressed as mean \pm SEM (n=4).

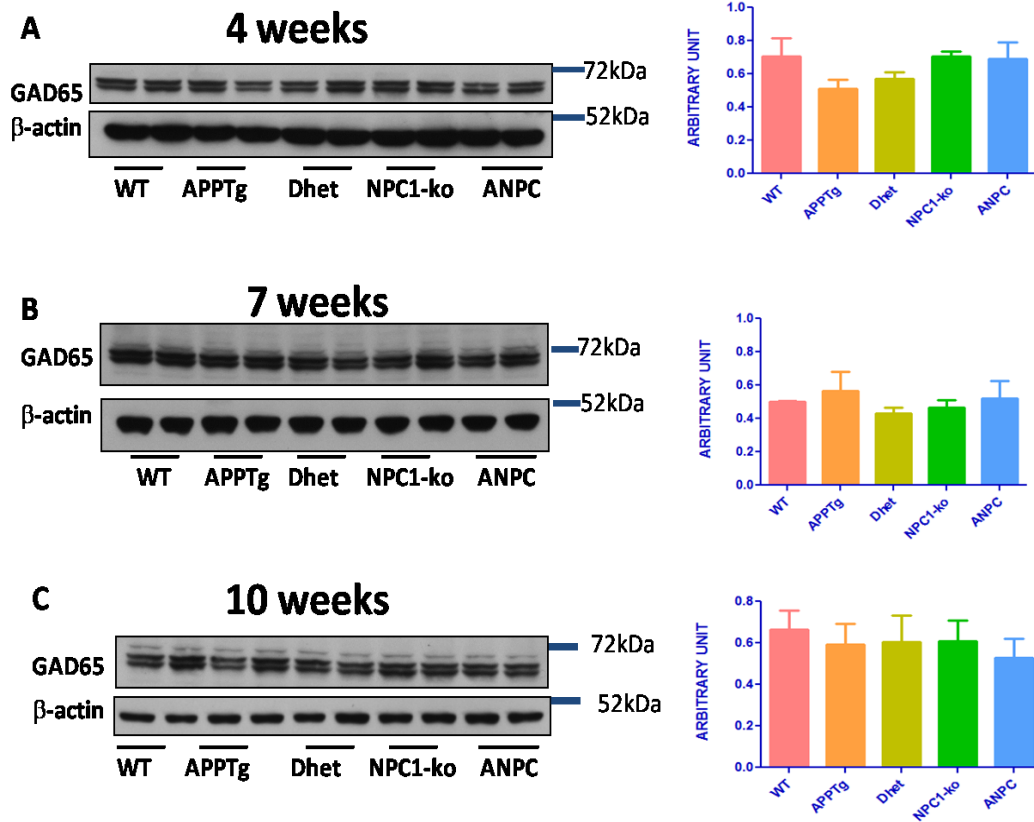


Fig 8: Western blots and corresponding histograms showing the levels of GAD65 in the cerebellum of the ANPC mice compared to other littermates at 4 (A), 7 (B) and 10 (C) weeks of age. Note that quantitative analysis showed no alterations in the level of GAD65 in the ANPC mice at any the time points with respect to the WT, APP-Tg, Dhet and NPC1-ko mice. Data are expressed as mean \pm SEM (n=4).

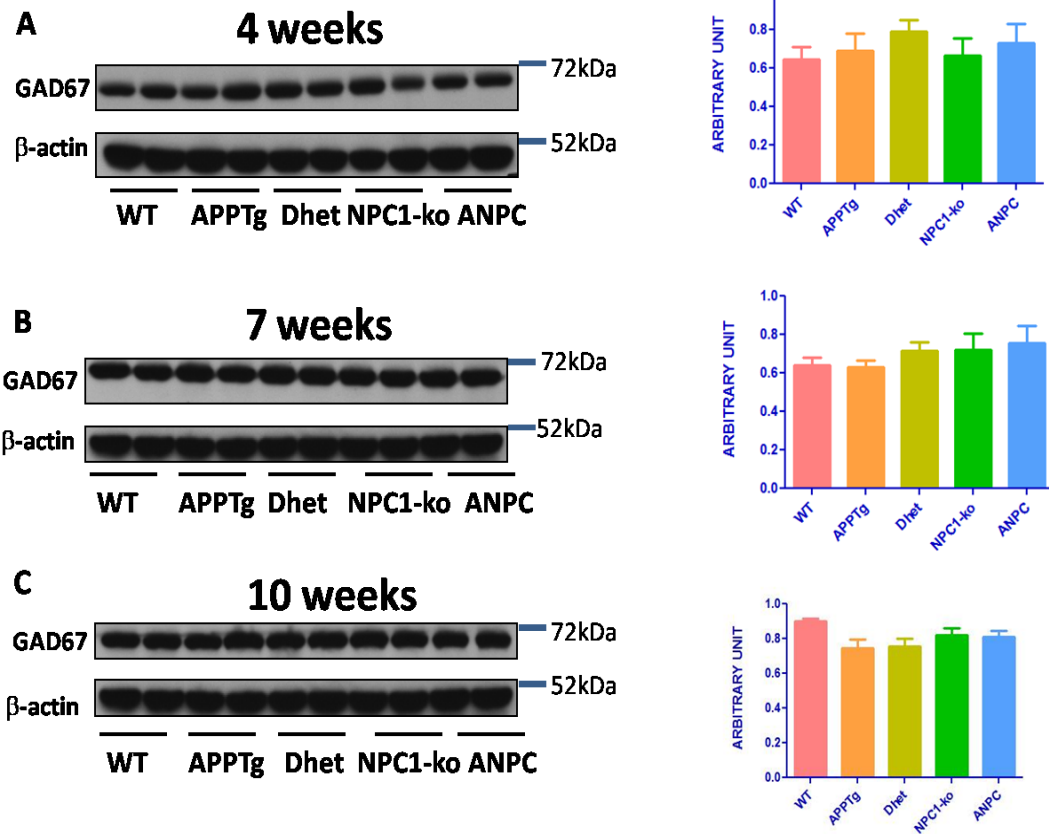


Fig 9: Western blots and corresponding histograms showing the levels of GAD67 in the frontal cortex of the ANPC mice compared to other littermates at 4 (A), 7 (B) and 10 (C) weeks of age. Note that quantitative analysis showed no alterations in the level of GAD67 in the ANPC mice at any the time points with respect to the WT, APP-Tg, Dhet and NPC1-ko mice. Data are expressed as mean \pm SEM (n=4).

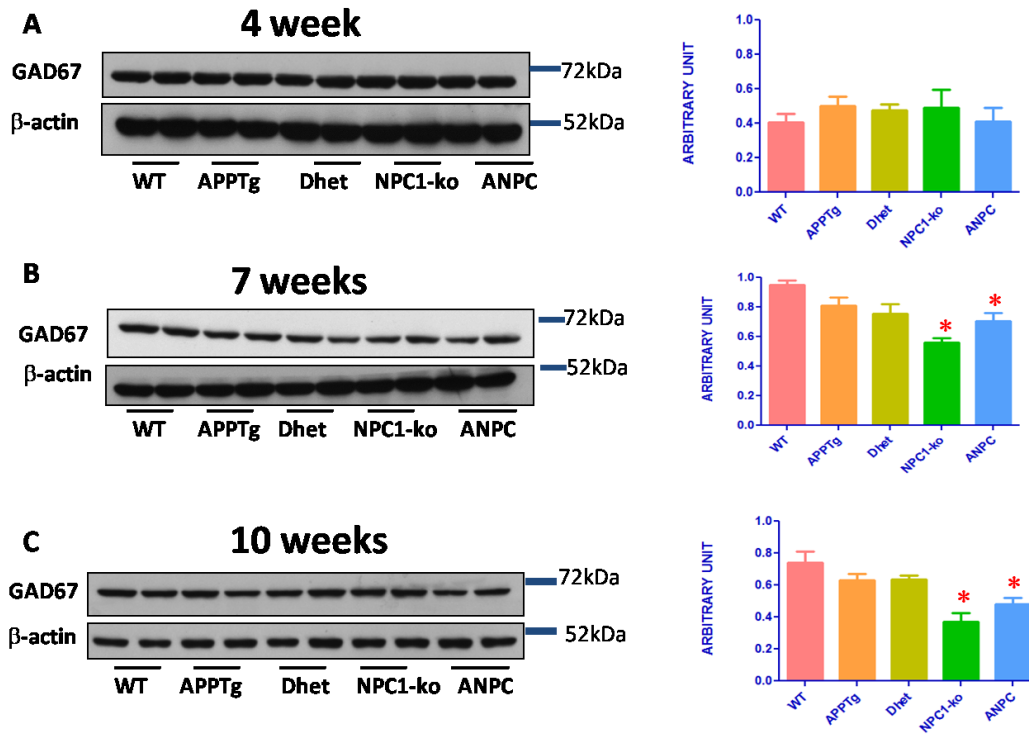


Fig 10: Western blots and corresponding histograms showing the levels of GAD67 in the cerebellum of the ANPC mice compared to other littermates at 4 (A), 7 (B) and 10 (C) weeks of age. Note that quantitative analysis showed significant decreases in the level of GAD67 in the ANPC and NPC1-ko mice at 7 and 10 weeks of age with respect to WT, APP-Tg and Dhet mice. Data are expressed as mean \pm SEM and * $p < 0.05$ (n=4).

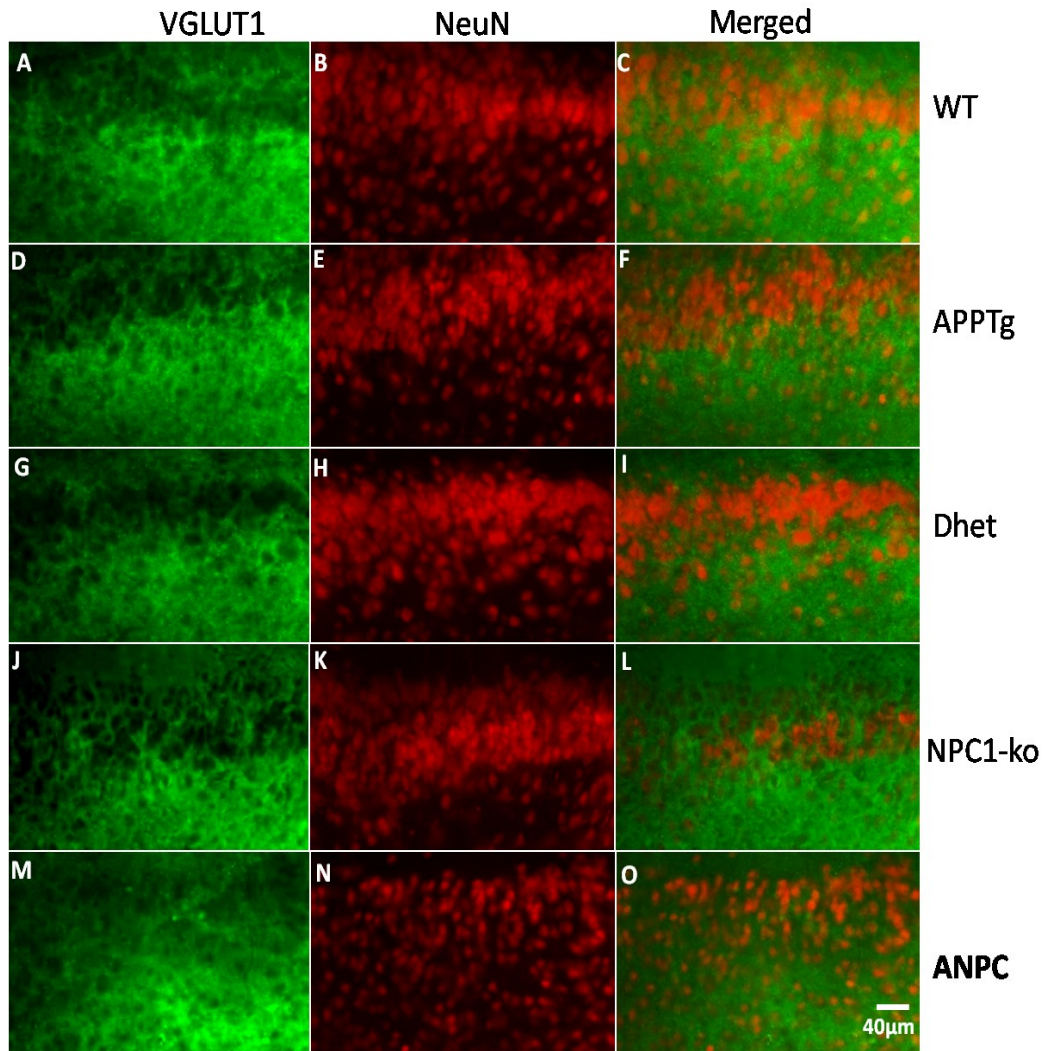


Fig 11: Double immunofluorescence photomicrographs showing the localization of VGLUT1 (green) and neuronal marker NeuN (red) in the frontal cortex of ANPC (M-O) mice compared to WT (A-C), APP-Tg (D-F), Dhet (G-I) and NPC1-ko (J-L) mice at 4 weeks of age. Note the decreased intensity of VGLUT1 staining in ANPC mice compared to other lines of mice.

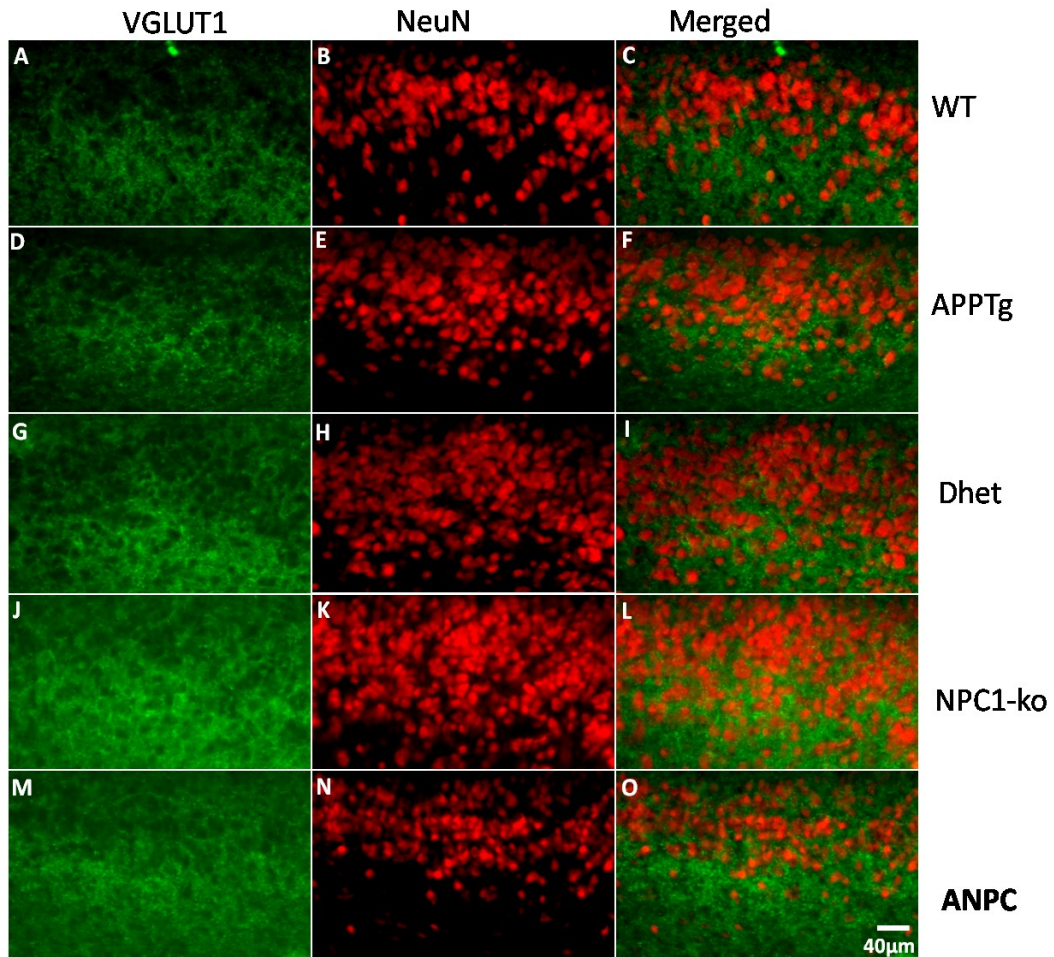


Fig 12: Double immunofluorescence photomicrographs showing the localization of VGLUT1 (green) and neuronal marker NeuN (red) in the frontal cortex of ANPC (M-O) mice compared to WT (A-C), APP-Tg (D-F), Dhet (G-I) and NPC1-ko (J-L) mice at 10 weeks of age. Note the decreased intensity of VGLUT1 staining in ANPC mice compared to other lines of mice.

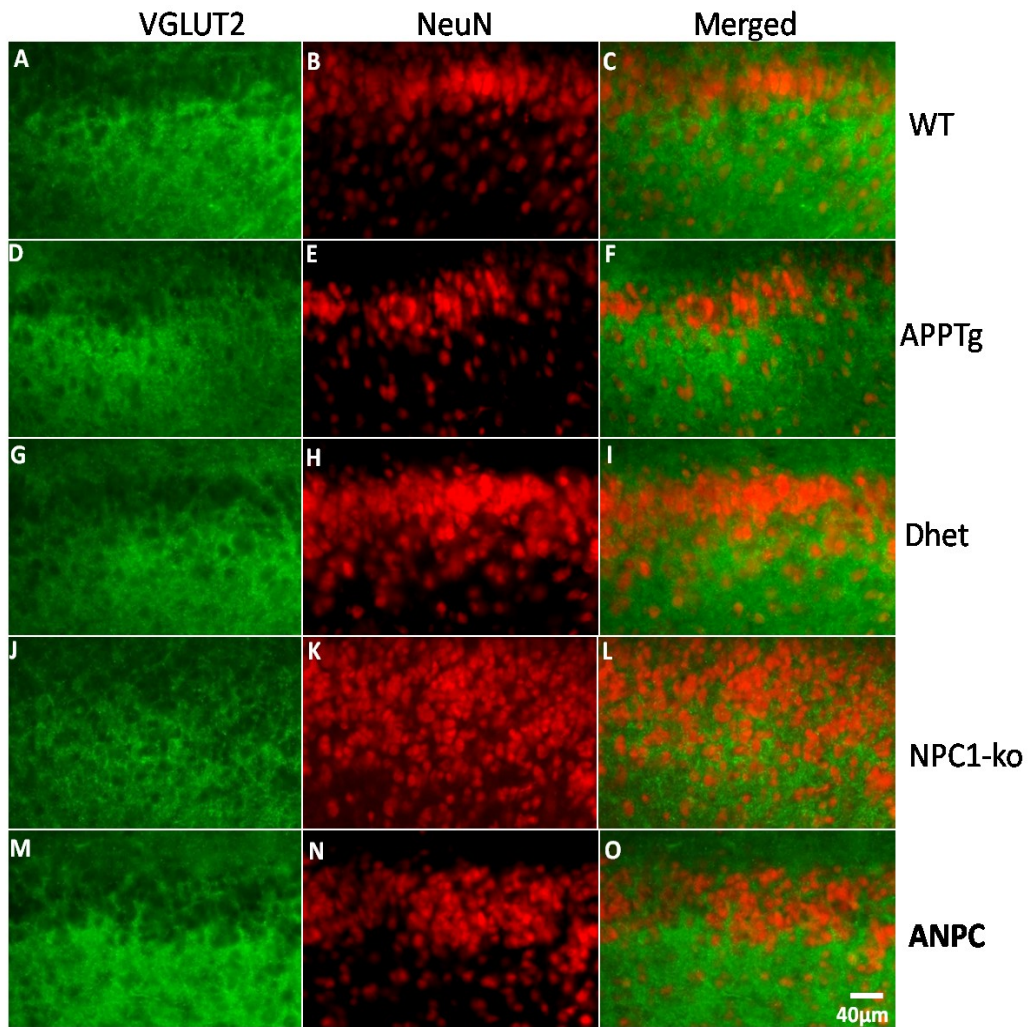


Fig 13: Double immunofluorescence photomicrographs showing the localization of VGLUT2 (green) and neuronal marker NeuN (red) in the frontal cortex of ANPC (M-O) mice compared to WT (A-C), APP-Tg (D-F), Dhet (G-I) and NPC1-ko (J-L) mice at 4 weeks of age. Note the decreased intensity of VGLUT2 staining in ANPC mice compared to other lines of mice.

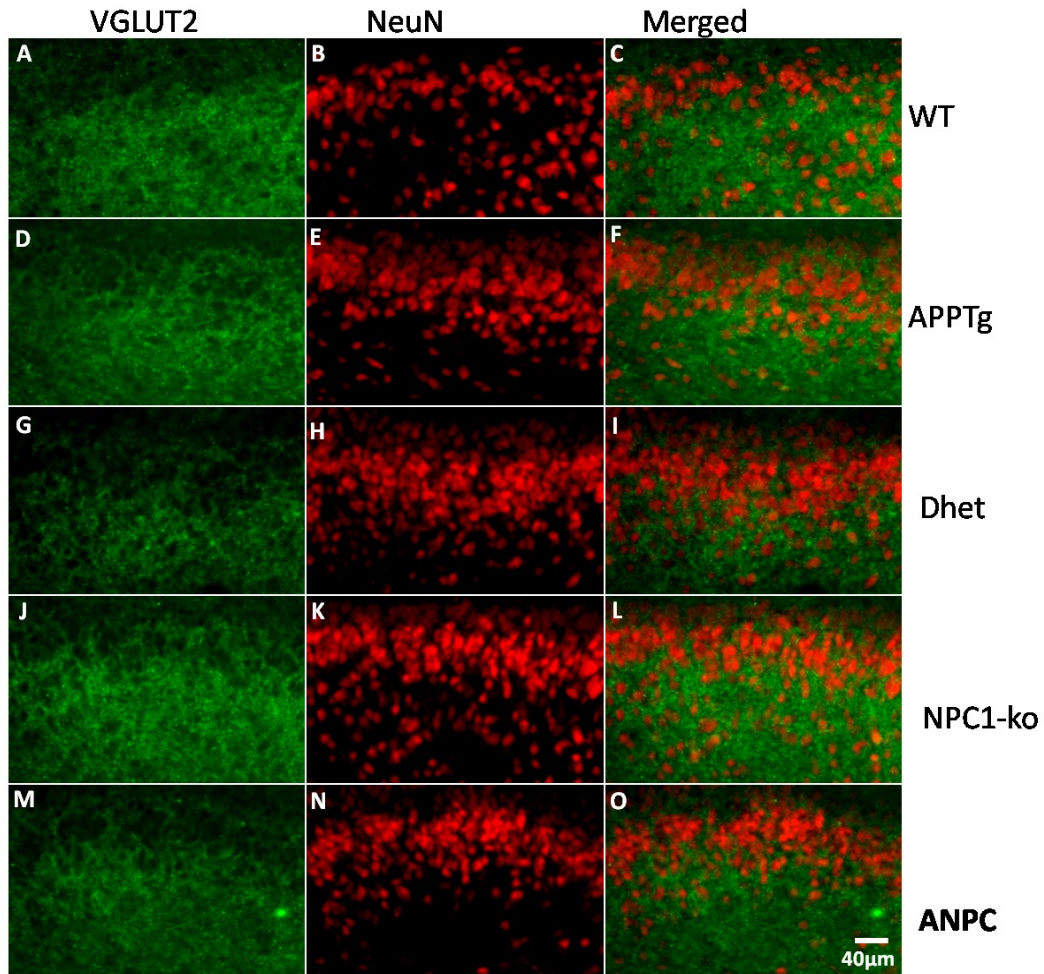


Fig 14: Double immunofluorescence photomicrographs showing the localization of VGLUT2 (green) and neuronal marker NeuN (red) in the frontal cortex ANPC (M-O) mice compared to WT (A-C), APP-Tg (D-F), Dhet (G-I) and NPC1-ko (J-L) mice at 10 weeks of age. Note the decreased intensity of VGLUT2 staining in ANPC mice compared to other lines of mice.

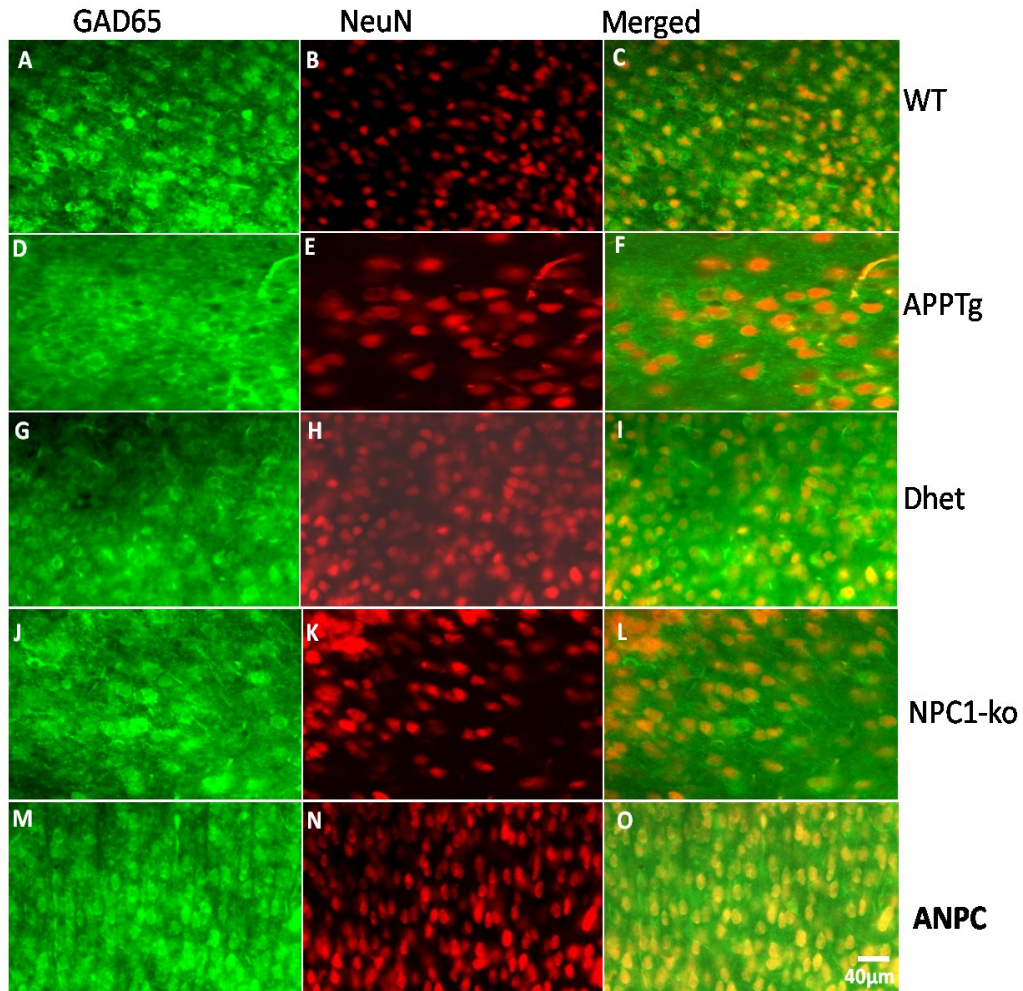


Fig 15: Double immunofluorescence photomicrographs showing the localization of GAD65 (green) and neuronal marker NeuN (red) in the frontal cortex of ANPC (M-O) mice compared to WT (A-C), APP-Tg (D-F), Dhet (G-I) and NPC1-ko (J-L) mice at 4 weeks of age. No apparent change in the intensity of GAD65 staining was evident in ANPC mice compared to other lines of mice.

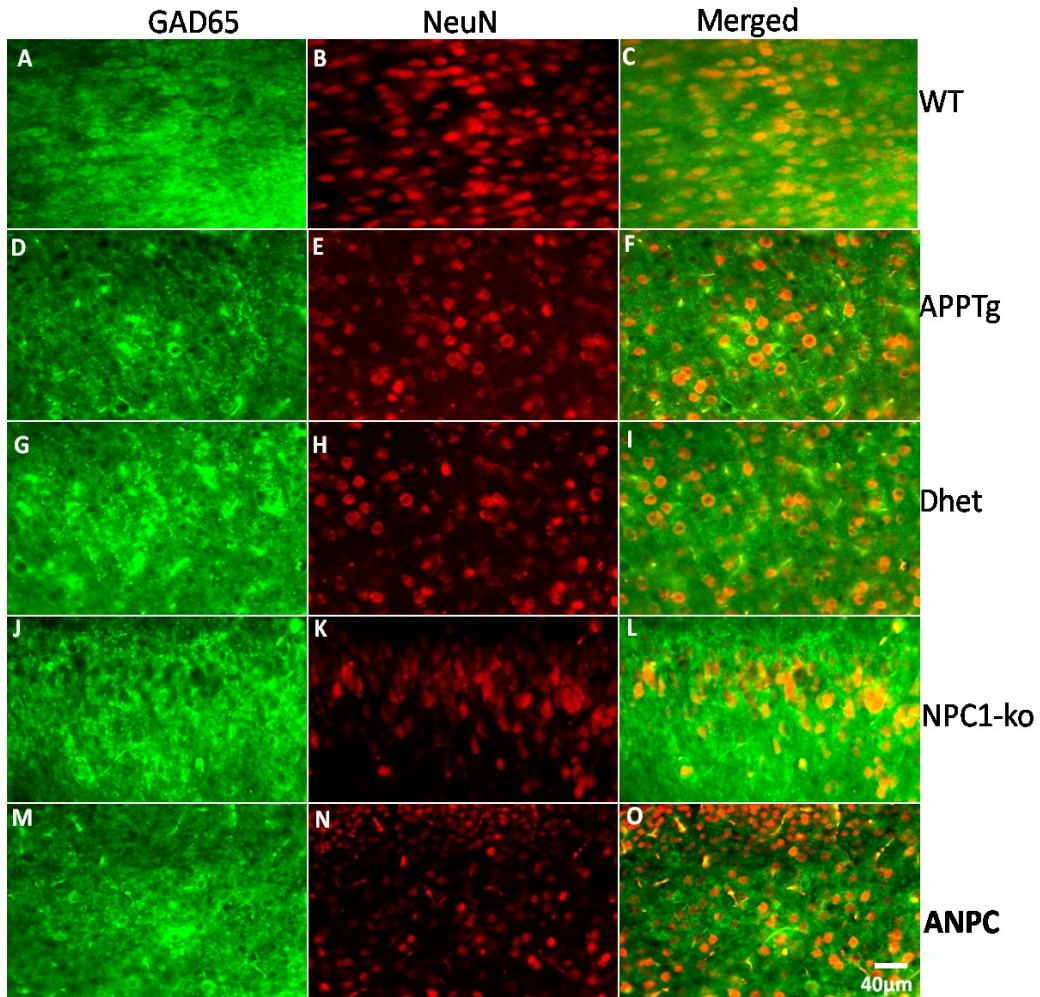


Fig 16: Double immunofluorescence photomicrographs showing the localization of GAD65 (green) and neuronal marker NeuN (red) in the frontal cortex of ANPC (M-O) mice compared to WT (A-C), APP-Tg (D-F), Dhet (G-I) and NPC1-ko (J-L) mice at 10 weeks of age. No apparent change in the intensity of GAD65 staining was evident in ANPC mice compared to other lines of mice.

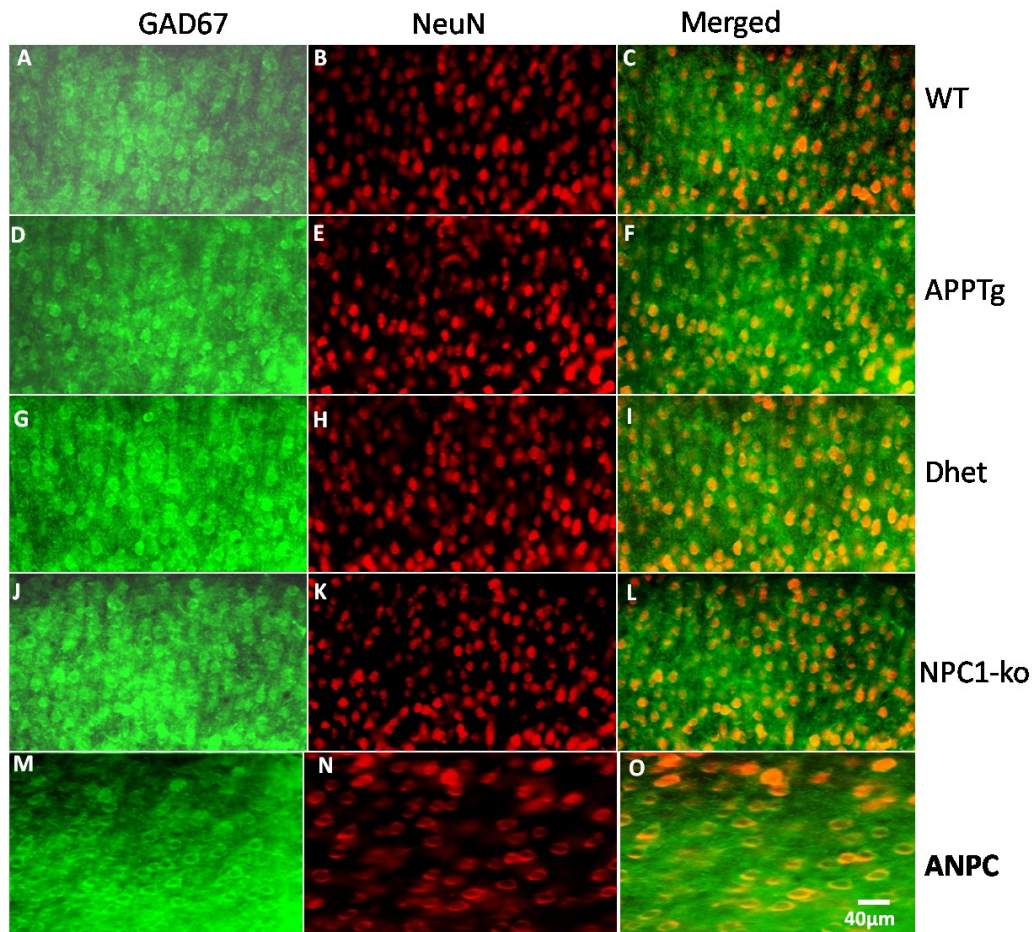


Fig 17: Double immunofluorescence photomicrographs showing the localization of GAD67 (green) and neuronal marker NeuN (red) in the frontal cortex of ANPC (M-O) mice compared to WT (A-C), APP-Tg (D-F), Dhet (G-I) and NPC1-ko (J-L) mice at 4 weeks of age. No apparent change in the intensity of GAD67 staining was evident in ANPC mice compared to other lines of mice.

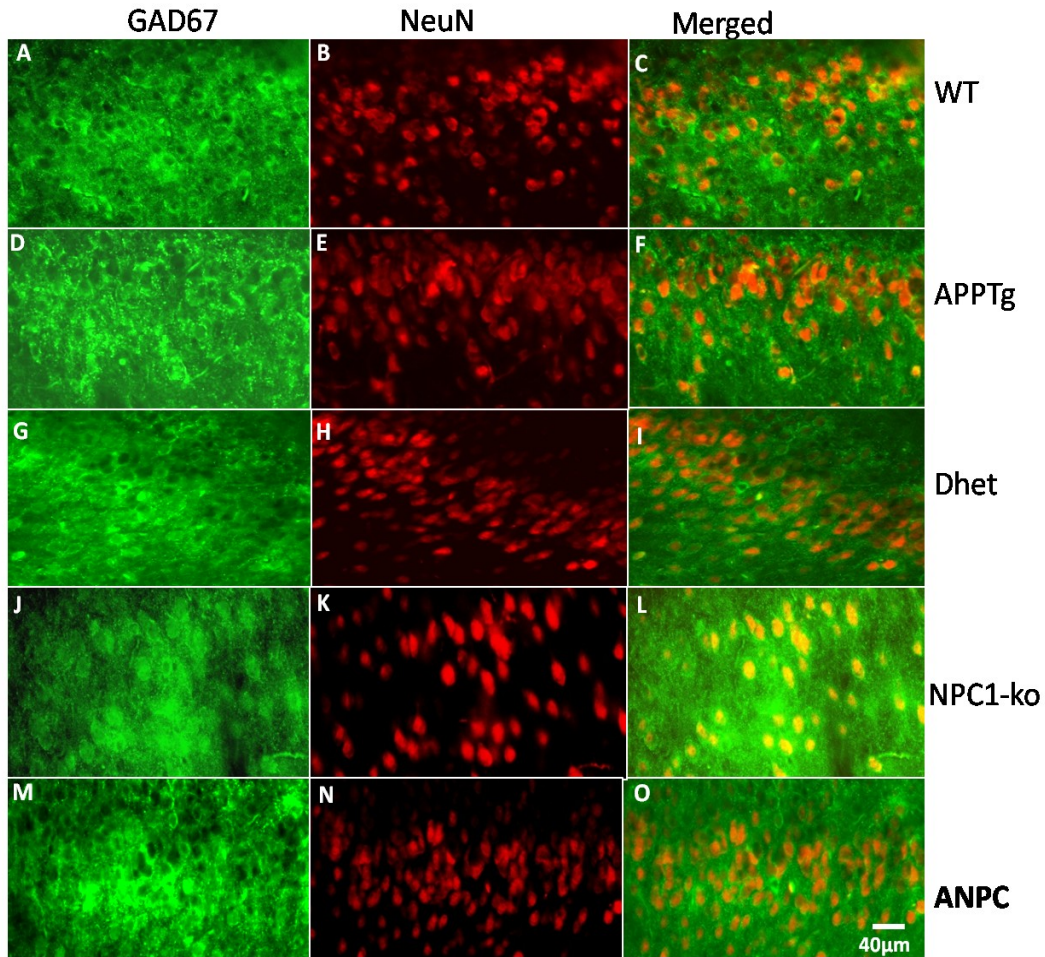


Fig 18: Double immunofluorescence photomicrographs showing the localization of GAD67 (green) and neuronal marker NeuN (red) in the frontal cortex of ANPC (M-O) mice compared to WT (A-C), APP-Tg (D-F), Dhet (G-I) and NPC1-ko (J-L) mice at 10 weeks of age. No apparent change in the intensity of GAD67 staining was evident in ANPC mice compared to other lines of mice.

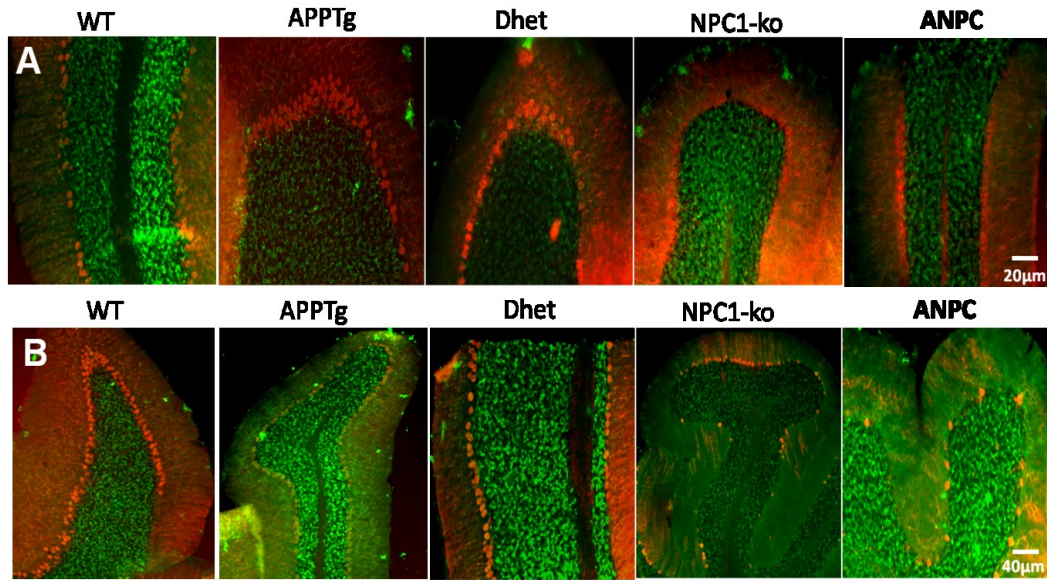


Fig 19: Double immunofluorescence photomicrographs showing the localization of VGLUT1 (green) and calbindin D-28 (red) labelled Purkinje neurons in the cerebellum of ANPC mice compared to WT, APP-Tg, Dhet and NPC1-ko mice at 4 weeks (A) and 10 weeks (B) of age. Note the decreased intensity of VGLUT1 staining in ANPC and NPC1-ko mice compared to other lines of mice.

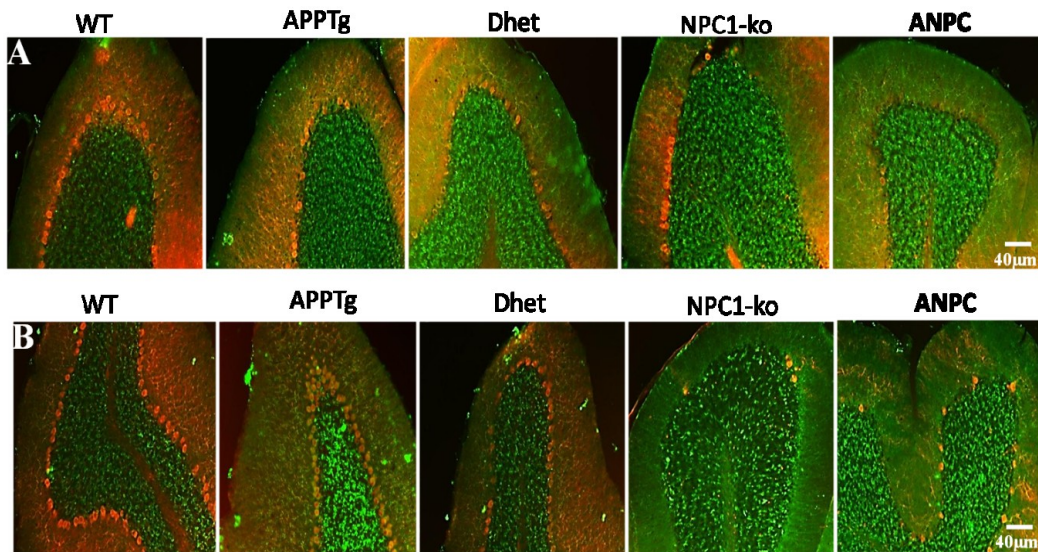


Fig 20: Double immunofluorescence photomicrographs showing the localization of VGLUT2 (green) and calbindin D-28 (red) labelled Purkinje neurons in the cerebellum of ANPC mice compared to WT, APP-Tg, Dhet and NPC1-ko mice at 4 weeks (A) and 10 weeks (B) of age. No apparent alteration in VGLUT2 immunoreactivity was evident in ANPC and NPC1-ko mice compared to other lines of mice.

4. Discussion

In our study we observed a lot of subtle but interesting changes in the glutamatergic and GABAergic systems in the frontal cortex and cerebellum of the ANPC mice compared to the WT, APP-Tg, Dhet and NPC1-ko mice. From these results it became evident that VGLUT1 levels are significantly decreased in the frontal cortex of the ANPC mice at 4, 7 and 10 weeks of age compared to other lines of mice. In the cerebellum, VGLUT1 and GAD67 levels were found to be significantly reduced in the ANPC mice compared to the age-matched WT, APP-Tg, Dhet and NPC1-ko mice at 7 and 10 weeks of age. VGLUT2 and GAD65 levels were unaltered in both frontal cortex and cerebellum of the ANPC mice at any age group compared to the other lines of mice; however GAD67 levels remained unaltered only in the frontal cortex of the ANPC mice compared to the other lines of mice. Intriguingly, our HPLC data did not reveal any alterations in the glutamate and GABA levels either in the frontal cortex or cerebellum of the ANPC mice at any age group compared to the other lines of mice. However, from our immunohistochemical studies, VGLUT1 and VGLUT2 immunoreactive puncta appeared to be less intense in 4 and 10 weeks old ANPC mice in comparison with WT, APP-Tg, Dhet and NPC1-ko mice in the frontal cortex. In the cerebellum, it was observed that with the progression of the disease pathology, both ANPC and NPC1-ko mice exhibit degeneration of the Purkinje cell layer by 10 weeks of age, causing a loss of VGLUT1 and VGLUT2 immunostaining in these mice compared to the WT, APP-Tg and Dhet mice. These results combined together suggest that intracellular accumulation of cholesterol along with overexpression of APP may influence glutamatergic and GABAergic systems in a subtle way in selected regions in the brain.

Cholesterol has long been linked with the incidence and the pathology of AD. To determine the effect of cholesterol on AD pathology our lab has recently developed a novel mouse model exhibiting intracellular cholesterol accumulation due to loss of functional Npc1 protein along with overexpression of mutant

human APP. These mice show cholesterol accumulation, aggravated glial pathology, deposition of A β plaques, tau hyperphosphorylation, loss of cognitive and motor functions and a life expectancy of not more than 70 days. These data suggested that cholesterol may play a crucial role in the progression of the AD pathology in these mice and can contribute to the severe phenotype that is found in these mice. But for the proper characterization and relevance of this model, it was important to study the effect of the disease pathology on the neurotransmitter systems in the brains of these mice. Since the glutamatergic and the GABAergic systems are major neurotransmitter systems in the CNS, we have measured the influence of cholesterol accumulation and APP over-expression in this new line of ANPC mice.

In the present study, we considered two main regions of the brain; frontal cortex and cerebellum. In AD, cerebral cortex and hippocampus are the two major areas of the brain which are affected (Coyle, Price, & DeLong, 1983). On the other hand, the brain region mostly affected in NPC disease is the cerebellum (Chang et al., 2005). In our ANPC mice, loss of the Purkinje cell layer was observed in the cerebellum but as with most other mutant APP transgenic mice (Maulik et al., 2012), we did not observe any significant loss of neurons either in the hippocampus or cerebral cortex. As both the frontal cortex and cerebellum are important for AD and NPC pathology respectively, the changes in the neurotransmitter systems were studied in these regions. The major finding that came out from our results is the significant decrease in the steady-state VGLUT1 levels in the ANPC mice compared to the WT, APP-Tg and the Dhet mice. VGLUT1 has been implicated in a number of well defined functions including the regulation of the quantal size and the release of glutamate per vesicle during excitatory synaptic transmission (Wilson et al., 2005). A small current is generated when a synaptic vesicle discharges its content of neurotransmitter onto the postsynaptic receptor patch at a fast chemical synapse which is termed as “quantal current.” The size of this quantal event varies among synapses and also at an individual synapse and is referred to as the quantal size (Karunanithi et al.,

2002). It has been shown that VGLUT1 can exploit receptor non-saturation at the scale of single vesicles through a shift in the glutamate concentration at the synaptic cleft. Moreover, VGLUT1 expression, apart from enhancing the amount of glutamate deposited per released event, also has the potential to control the likelihood of that release event to occur (Wilson et al., 2005). The strength of synaptic transmission is controlled both at the pre- and post-synaptic levels. It is suggested that glutamate receptors are generally far from being saturated during quantal transmission (Yamashita et al., 2003). In that case small variations of glutamate concentration in the synaptic cleft could contribute significantly to the variability of the excitatory current. Glutamate concentration in the synaptic cleft depends not only on the number of synaptic vesicles and the vesicular concentration of glutamate but also on the changes in the activity of the vesicular transporters (Williams, 1997). Only a small portion of synaptic vesicles are directly involved at the active zone of the synapse. Consequently, after exocytotic release of the neurotransmitter, these active vesicles have to rapidly reload glutamate for the next release (Murthy & Stevens, 1999). These reflect the essential role of VGLUTs in glutamatergic neurotransmission. A decrease in the levels of VGLUT1 in the cortex of ANPC mice starting from 4 weeks of age may suggest a progressive lack of glutamatergic neurotransmission and also a decrease in the glutamatergic quantal size. Loss of VGLUT1 expression has been reported to substantially deplete the pool of synaptic vesicles at excitatory terminals (Fremeau et al., 2001). In this context, we also see a decrease in the glutamatergic bouton density in the cortical sections of ANPC mice compared to the other lines of mice both at 4 and 10 weeks age. Thus, it can be concluded that there may be a decrease in the synaptic vesicles containing VGLUT1 which in turn can affect the glutamatergic neurotransmission. Interestingly, the endogenous levels of glutamate, i.e. the total content of glutamate in the cortex, did not exhibit significant alterations in ANPC mice compared to other lines of mice. This suggests that though there may be a lack of glutamatergic neurotransmission in the synaptic cleft, the total pool of glutamate (which includes both metabolic as well as transmitter pools) in the brain is not altered. A probable reason may be the

presence of a large number of glial glutamatergic transporters. The numbers of astrocytes, which are the primary uptake sites of glutamate, are found to be increased significantly along with the microglia in the ANPC mice from 4 weeks onwards. This may suggest that the proliferation/activation of the astrocytes in the ANPC mice may increase the activity of the glial glutamatergic transporters such as excitatory amino acid transporter1-5 which in turn increases the uptake of glutamate in the astrocytes from the neurons and compensates for the lack of VGLUT1 specific glutamatergic neurotransmission and thus maintains a constant pool of glutamate. In the ANPC mice, the expression level of VGLUT1 decreases in the cerebellum as the pathology progresses. At 10 weeks, which is the terminal stage for the ANPC mice, very low amounts of VGLUT1 were detected by western blotting, suggesting a depleted role of glutamatergic transmission which may underlie the severe phenotype found in these mice.

Interestingly, in contrast to VGLUT1, the expression level of VGLUT2 was found to be unaltered in the cortex of ANPC mice compared to the other lines of mice. Thus, it seems likely that VGLUT1 and VGLUT2 may work independently. This is supported by the evidence that climbing fibers exclusively use VGLUT2, whereas the parallel fibers only employ VGLUT1 for vesicular glutamate uptake in the molecular layer of the cerebellar cortex (Fremeau et al., 2001; Murthy & Stevens, 1999). However, both VGLUT1 and VGLUT2 were also found to be co-localized in single mossy-fiber terminals (Hioki et al., 2003). It is reported that VGLUT2 is involved in early brain development and in controlling the neurons responsible for basic functions of respiration and those involved in the autonomic nervous system. Lack of VGLUT2 may cause neuropathic pain. Like VGLUT1, VGLUT2 also controls the release of glutamate from the neurons (Moechars et al., 2006). The presence of normal amounts of VGLUT2 in the cortex of ANPC mice raises the possibility that the function of certain populations of neurons that contain VGLUT2 may not be altered, whereas the population of neurons containing VGLUT1 may be altered.

In the cerebellum of the ANPC mice, VGLUT1 levels were found to be decreased with the progression of disease pathology. The levels at 4 weeks were unaltered in the ANPC mice compared to the other lines of mice. But at 7 weeks of age, as the disease pathology became severe, we observed a significant decrease in the levels of VGLUT1 in the ANPC mice with respect to WT, APP-Tg and Dhet mice. At 10 weeks of age this decrease got even more pronounced. But unlike the frontal cortex, VGLUT1 levels in the cerebellum are also found to be significantly reduced in the NPC1-ko mice, compared to the WT, APP-Tg and Dhet mice at 7 and 10 weeks of age. VGLUT1 reduction in the cerebellum of these mice may be related to the loss of Purkinje neurons. In the cerebellum, the Purkinje cells form synapses with the parallel fibers expressing VGLUT1 protein. In the absence of the Purkinje layer, these synapses are possibly destroyed, which may lead to a reduction in the VGLUT1 protein levels. Sometimes, these synapses coincide with the synapses formed between the climbing fibers expressing VGLUT2 protein and the Purkinje cells. From the immunohistochemical data it is evident that there is also a loss of VGLUT1- and VGLUT2-expressing boutons in the molecular layer of the cerebellum adjacent to the Purkinje layer. However, VGLUT2 protein levels in the ANPC and NPC1-ko mice remain unaltered in comparison with other genotypes. This may be due to an increased expression of VGLUT2 in the granular layer of the cerebellum where we observed a dense staining in all lines of mice. It can be suggested that the VGLUT2 levels in the granular layer of the cerebellum compensated for the lack of VGLUT2 immunostaining in the molecular layer to cause no decrease in the overall protein levels. Thus, there is a decrease in the levels of VGLUT1, but not VGLUT2, in the cerebellum of the ANPC and NPC1-ko mice compared to the other lines. This may be involved in regulating the functional abnormalities associated with the cerebellum of ANPC and NPC1-ko mice.

In contrast to the VGLUT1 levels, it was observed that neither the total content of GABA nor the expression levels of its synthesizing enzymes GAD65 and GAD67 were altered in the cortex of the ANPC mice compared to the WT, APP-Tg, Dhet

and NPC1-ko mice. Moreover, there was no visible loss of neurons in the cortex of these mice. These results suggest that in the cortex, the disease pathology may not be severe enough to affect the normal functioning of GABAergic neurotransmission. In the cerebellum, however, there was a progressive decrease in the levels of GAD67 in both the ANPC and NPC1-ko mice compared to the WT, APP-Tg and Dhet mice. In ANPC and NPC1-ko mice, it was evident that there is loss of the Purkinje neurons starting from 7 weeks of age (Maulik et al., 2012). At 4 weeks of age, the Purkinje cell layer is completely intact, but at 10 weeks of age this cell layer completely disappeared in both ANPC and NPC1-ko mice. The Purkinje neurons are the major GABAergic neurons in the cerebellum. They are found to have high levels of GAD67, whereas GAD65 is mostly present in the nerve terminals and dendrites (Esclapez et al., 1994). In the absence of Purkinje neurons, the GAD67 level was also found to be decreased. In the mammalian cerebellum, Purkinje, stellate, basket and Golgi cells are inhibitory neurons that release GABA as neurotransmitter (Ottersen, 1993). GAD67 is predominantly present in the Purkinje cells, whereas GAD65 is present mostly in the stellate, basket and Golgi cells. In the cerebellum of the ANPC and NPC1-ko mice there is loss of Purkinje neurons and not the other GABAergic neurons, which may account for the unaltered protein expression of GAD65 in the cerebellum. It has been suggested that GAD67 is mainly responsible for the synthesis of GABA, whereas GAD65 is involved in regulating GABAergic-transmission. In mice lacking GAD67, the morphology of Purkinje neurons and the density of synaptic terminals in the cerebellar cortex appeared unaffected. It was suggested that this lack of alteration in the Purkinje neurons and synaptic density was due to the presence of high amounts of GAD65 (Obata et al., 2008). The cerebellar GABA level in the GAD67-ko mice was reduced to 16–44% of the normal level. This was supposedly due to the presence of the GAD65 isoform. This suggests that GAD65 not only helps in GABAergic neurotransmission but also in synthesis of GABA in the absence of the GAD67 isoform (Kawaguchi, 2010). Similarly, in the case of NPC1-ko and ANPC mice, due to the decrease in the level of GAD67 and in the absence of the Purkinje neurons, GAD65 present in

the other cerebellar cell types such as stellate, basket and Golgi cells may contribute to the synthesis and transmission of GABA and maintain the GABA pool in the cerebellum. This supports our HPLC data which show no alteration in the endogenous levels of GABA in the ANPC and NPC1-ko mice compared to the other lines of mice.

Loss of VGLUT1 has been correlated to cognitive impairment in AD patients. It was shown that loss of VGLUT1 coincided with cognitive impairment observed in mild to moderate dementia patients. However, there was no correlation between VGLUT1 levels and the normal aging process (Kashani et al., 2008). It is evident from other studies that VGLUT1 may be correlated with depression. Mice with reduced expression of VGLUT1 showed enhanced anxiety, depressive symptoms and impaired recognition memory (Tordera et al., 2007). Thus, in this context we suggest that VGLUT1 reduction in both the cortex and cerebellum can be a major factor contributing to the cognitive decline found in the ANPC mice starting from an early stage. Loss of glutamatergic neurotransmission in the brain may also lead to tardive dyskinesia or tremors in the body (Tsai et al., 1998). In the ANPC mice, visible tremors along with difficulty in movement were evident from as early as 4 weeks of age. These mice also show ataxia. These abnormalities may be due to the lack of VGLUT1-specific glutamatergic neurotransmission and/or the loss of GAD67-enriched Purkinje neurons in the cerebellum.

Thus, in this mouse model, cholesterol accumulation not only impacts the progression of the AD-related pathology, but also leads to subtle alterations in glutamatergic and GABAergic markers. In the ANPC mice, it is evident that there is a lack of VGLUT1-specific glutamatergic neurotransmission in both the frontal cortex and the cerebellum. This in turn may contribute to a number of factors including small body size, motor and cognitive impairment and early death of these mice. Glutamatergic neurotransmission may also lead to oxidative stress which is a crucial factor in the AD pathology. Though from the scope of this

study all these factors cannot be confirmed, the results suggest that the loss of VGLUT1 and GAD67 may play a crucial role. To prove the effect of these changes on the neurotransmission, glutamate and GABA release can be measured in the future, which may shed light on the functional status of these neurons. In both glutamatergic and GABAergic neurotransmission, different ionotropic and metabotropic receptors play a pivotal role. In this context, future experiments can also be performed to investigate the changes in the glutamate receptors and their various subunits. The changes in the receptors may be evaluated with the help of specific antibodies directed towards the various subunits or by the use of different ligand binding assays. This will in turn shed more light in the differential distribution and transmission of both the glutamatergic and GABAergic signals. As suggested by previous studies, even the slightest change in the levels of the receptors and/or their subunit or differential distribution profile may lead to substantial alterations in the glutamatergic and GABAergic neurotransmission pathways (Dingledine et al., 1999; Lujan et al., 2005). So, measuring the levels of these various receptors may provide conclusive evidence of the disruption of proper neurotransmission. Though this study gives us some idea about the changes in the neurotransmitter markers, further detailed study is needed to confirm the effects of the imbalance in these systems.

5. References

- Alloul, K., Sauriol, L., Kennedy, W., Laurier, C., Tessier, G., Novosel, S., et al. (1998). Alzheimer's disease: A review of the disease, its epidemiology and economic impact. *Archives of Gerontology and Geriatrics*, 27(3), 189-221.
- Auer, I. A., Schmidt, M. L., Lee, V. M., Curry, B., Suzuki, K., Shin, R. W., et al. (1995). Paired helical filament tau (PHFtau) in Niemann-Pick type C disease is similar to PHFtau in Alzheimer's disease. *Acta Neuropathologica*, 90(6), 547-551.
- Awapara, J., Landua, A. J., Fuerst, R., & Seale, B. (1950). Free gamma-aminobutyric acid in brain. *The Journal of Biological Chemistry*, 187(1), 35-39.
- Ayalon, G., & Stern-Bach, Y. (2001). Functional assembly of AMPA and kainate receptors is mediated by several discrete protein-protein interactions. *Neuron*, 31(1), 103-113.
- Beffert, U., Cohn, J. S., Petit-Turcotte, C., Tremblay, M., Aumont, N., Ramassamy, C., et al. (1999). Apolipoprotein E and beta-amyloid levels in the hippocampus and frontal cortex of Alzheimer's disease subjects are disease-related and apolipoprotein E genotype dependent. *Brain Research*, 843(1-2), 87-94.
- Bjorkhem, I., & Meaney, S. (2004). Brain cholesterol: Long secret life behind a barrier. *Arteriosclerosis, Thrombosis, and Vascular Biology*, 24(5), 806-815.
- Blacker, D. (1997). The genetics of Alzheimer's disease: Progress, possibilities, and pitfalls. *Harvard Review of Psychiatry*, 5(4), 234-237.
- Blacker, D., Haines, J. L., Rodes, L., Terwedow, H., Go, R. C., Harrell, L. E., et al. (1997). ApoE-4 and age at onset of Alzheimer's disease: The NIMH genetics initiative. *Neurology*, 48(1), 139-147.
- Bodovitz, S., & Klein, W. L. (1996). Cholesterol modulates alpha-secretase cleavage of amyloid precursor protein. *The Journal of Biological Chemistry*, 271(8), 4436-4440.
- Bormann, J. (1988). Electrophysiology of GABAA and GABAB receptor subtypes. *Trends in Neurosciences*, 11(3), 112-116.
- Bormann, J., & Feigenspan, A. (1995). GABAC receptors. *Trends in Neurosciences*, 18(12), 515-519.
- Boyles, J. K., Zoellner, C. D., Anderson, L. J., Kosik, L. M., Pitas, R. E., Weisgraber, K. H., et al. (1989). A role for apolipoprotein E, apolipoprotein A-I,

and low density lipoprotein receptors in cholesterol transport during regeneration and remyelination of the rat sciatic nerve. *The Journal of Clinical Investigation*, 83(3), 1015-1031.

Braak, H., & Braak, E. (1991). Demonstration of amyloid deposits and neurofibrillary changes in whole brain sections. *Brain Pathology*, 1(3), 213-216.

Butterfield, D. A., Hensley, K., Cole, P., Subramaniam, R., Aksenov, M., Aksenova, M., et al. (1997). Oxidatively induced structural alteration of glutamine synthetase assessed by analysis of spin label incorporation kinetics: Relevance to Alzheimer's disease. *Journal of Neurochemistry*, 68(6), 2451-2457.

Byun, K., Kim, J., Cho, S. Y., Hutchinson, B., Yang, S. R., Kang, K. S., et al. (2006). Alteration of the glutamate and GABA transporters in the hippocampus of the Niemann-Pick disease, type C mouse using proteomic analysis. *Proteomics*, 6(4), 1230-1236.

Carstea, E. D., Morris, J. A., Coleman, K. G., Loftus, S. K., Zhang, D., Cummings, C., et al. (1997). Niemann-Pick C1 disease gene: Homology to mediators of cholesterol homeostasis. *Science (New York, N.Y.)*, 277(5323), 228-231.

Carstea, E. D., Polymeropoulos, M. H., Parker, C. C., Detera-Wadleigh, S. D., O'Neill, R. R., Patterson, M. C., et al. (1993). Linkage of Niemann-Pick disease type C to human chromosome 18. *Proceedings of the National Academy of Sciences of the United States of America*, 90(5), 2002-2004.

Castano, E. M., Prelli, F. C., & Frangione, B. (1995). Apolipoprotein E and amyloidogenesis. *Laboratory Investigation; a Journal of Technical Methods and Pathology*, 73(4), 457-460.

Chang, T. Y., Reid, P. C., Sugii, S., Ohgami, N., Cruz, J. C., & Chang, C. C. (2005). Niemann-Pick type C disease and intracellular cholesterol trafficking. *The Journal of Biological Chemistry*, 280(22), 20917-20920.

Chen, F. W., Gordon, R. E., & Ioannou, Y. A. (2005). NPC1 late endosomes contain elevated levels of non-esterified ('free') fatty acids and an abnormally glycosylated form of the NPC2 protein. *The Biochemical Journal*, 390(Pt 2), 549-561.

Cherubini, E., & Conti, F. (2001). Generating diversity at GABAergic synapses. *Trends in Neurosciences*, 24(3), 155-162.

Chishti, M. A., Yang, D. S., Janus, C., Phinney, A. L., Horne, P., Pearson, J., et al. (2001). Early-onset amyloid deposition and cognitive deficits in transgenic mice

expressing a double mutant form of amyloid precursor protein 695. *The Journal of Biological Chemistry*, 276(24), 21562-21570.

Choi, D. W. (1988). Glutamate neurotoxicity and diseases of the nervous system. *Neuron*, 1(8), 623-634.

Citron, M., Diehl, T. S., Gordon, G., Biere, A. L., Seubert, P., & Selkoe, D. J. (1996). Evidence that the 42- and 40-amino acid forms of amyloid beta protein are generated from the beta-amyloid precursor protein by different protease activities. *Proceedings of the National Academy of Sciences of the United States of America*, 93(23), 13170-13175.

Corder, E. H., Saunders, A. M., Risch, N. J., Strittmatter, W. J., Schmechel, D. E., Gaskell, P. C., Jr, et al. (1994). Protective effect of apolipoprotein E type 2 allele for late onset alzheimer disease. *Nature Genetics*, 7(2), 180-184.

Cossette, P., Lachance-Touchette, P., & Rouleau G.A. (2012), Mutated GABA_A receptors subunits in idiopathic generalized epilepsy. In Jasper's Basic Mechanisms of the Epilepsies. 4th Edition, Noebels, J.L., Avoli, M., Rogawaski, M.A., Olsen, R.W., & Delgado-Escueta, A.V. (eds.), National Center of Biotechnology Information, Bethesda (MD).

Cotman, C. W., Geddes, J. W., Bridges, R. J., & Monaghan, D. T. (1989). N-Methyl-D-aspartate receptors and Alzheimer's disease. *Neurobiology of Aging*, 10(5), 603-5; discussion 618-20.

Coyle, J. T., Price, D. L., & DeLong, M. R. (1983). Alzheimer's disease: A disorder of cortical cholinergic innervation. *Science (New York, N.Y.)*, 219(4589), 1184-1190.

Danbolt, N. C. (2001). Glutamate uptake. *Progress in Neurobiology*, 65(1), 1-105.

Davies, P., & Maloney, A. J. (1976). Selective loss of central cholinergic neurons in Alzheimer's disease. *Lancet*, 2(8000), 1403.

De Boni, U., & McLachlan, D. R. (1985). Controlled induction of paired helical filaments of the alzheimer type in cultured human neurons, by glutamate and aspartate. *Journal of the Neurological Sciences*, 68(2-3), 105-118.

Dietschy, J. M., & Turley, S. D. (2004). Thematic review series: Brain lipids. cholesterol metabolism in the central nervous system during early development and in the mature animal. *Journal of Lipid Research*, 45(8), 1375-1397.

Dingledine, R., Borges, K., Bowie, D., & Traynelis, S. F. (1999). The glutamate receptor ion channels. *Pharmacological Reviews*, 51(1), 7-61.

- Esch, F. S., Keim, P. S., Beattie, E. C., Blacher, R. W., Culwell, A. R., Oltersdorf, T., et al. (1990). Cleavage of amyloid beta peptide during constitutive processing of its precursor. *Science (New York, N.Y.)*, 248(4959), 1122-1124.
- Esclapez, M., Tillakaratne, N. J., Kaufman, D. L., Tobin, A. J., & Houser, C. R. (1994). Comparative localization of two forms of glutamic acid decarboxylase and their mRNAs in rat brain supports the concept of functional differences between the forms. *The Journal of Neuroscience*, 14(3 Pt 2), 1834-1855.
- Fassbender, K., Simons, M., Bergmann, C., Stroick, M., Lutjohann, D., Keller, P., et al. (2001). Simvastatin strongly reduces levels of Alzheimer's disease beta - amyloid peptides abeta 42 and abeta 40 in vitro and in vivo. *Proceedings of the National Academy of Sciences of the United States of America*, 98(10), 5856-5861.
- Francis, P. T., Webster, M. T., Chessell, I. P., Holmes, C., Stratmann, G. C., Procter, A. W., et al. (1993). Neurotransmitters and second messengers in aging and Alzheimer's disease. *Annals of the New York Academy of Sciences*, 695, 19-26.
- Fremeau, R. T., Jr, Troyer, M. D., Pahner, I., Nygaard, G. O., Tran, C. H., Reimer, R. J., et al. (2001). The expression of vesicular glutamate transporters defines two classes of excitatory synapse. *Neuron*, 31(2), 247-260.
- Galbete, J. L., Martin, T. R., Peressini, E., Modena, P., Bianchi, R., & Forloni, G. (2000). Cholesterol decreases secretion of the secreted form of amyloid precursor protein by interfering with glycosylation in the protein secretory pathway. *The Biochemical Journal*, 348 Pt 2, 307-313.
- Garcia-Alloza, M., Tsang, S. W., Gil-Bea, F. J., Francis, P. T., Lai, M. K., Marcos, B., et al. (2006). Involvement of the GABAergic system in depressive symptoms of Alzheimer's disease. *Neurobiology of Aging*, 27(8), 1110-1117.
- Garver, W. S., Heidenreich, R. A., Erickson, R. P., Thomas, M. A., & Wilson, J. M. (2000). Localization of the murine Niemann-Pick C1 protein to two distinct intracellular compartments. *Journal of Lipid Research*, 41(5), 673-687.
- Gellermann, G. P., Ullrich, K., Tannert, A., Unger, C., Habicht, G., Sauter, S. R., et al. (2006). Alzheimer-like plaque formation by human macrophages is reduced by fibrillation inhibitors and lovastatin. *Journal of Molecular Biology*, 360(2), 251-257.
- Goedert, M. (1993). Tau protein and the neurofibrillary pathology of Alzheimer's disease. *Trends in Neurosciences*, 16(11), 460-465.

Gomez-Isla, T., Price, J. L., McKeel, D. W., Jr, Morris, J. C., Growdon, J. H., & Hyman, B. T. (1996). Profound loss of layer II entorhinal cortex neurons occurs in very mild Alzheimer's disease. *The Journal of Neuroscience*, *16*(14), 4491-4500.

Grabowski, T. J., & Damasio, A. R. (1996). Improving functional imaging techniques: The dream of a single image for a single mental event. *Proceedings of the National Academy of Sciences of the United States of America*, *93*(25), 14302-14303.

Grant, S. L., Shulman, Y., Tibbo, P., Hampson, D. R., & Baker, G. B. (2006). Determination of D-serine and related neuroactive amino acids in human plasma by high-performance liquid chromatography with fluorimetric detection. *Journal of Chromatography.B, Analytical Technologies in the Biomedical and Life Sciences*, *844*(2), 278-282.

Greenamyre, J. T., Penney, J. B., D'Amato, C. J., & Young, A. B. (1987). Dementia of the Alzheimer's type: Changes in hippocampal L-[³H] glutamate binding. *Journal of Neurochemistry*, *48*(2), 543-551.

Greenamyre, J. T., & Young, A. B. (1989). Excitatory amino acids and Alzheimer's disease. *Neurobiology of Aging*, *10*(5), 593-602.

Hannan, S., Wilkins, M.E., & Smart, T.G. (2012). Sushi domain confer distinct trafficking profiles on GABA_B receptors. *Proceedings of the National Academy of Sciences of the United States of America*, *109*(30), 12171-12176, doi:10.1073/pnas.1201660109.

Haass, C. (2004). Take five--BACE and the gamma-secretase quartet conduct Alzheimer's amyloid beta-peptide generation. *The EMBO Journal*, *23*(3), 483-488.

Hardy, J. (1997). Amyloid, the presenilins and Alzheimer's disease. *Trends in Neurosciences*, *20*(4), 154-159.

Hardy, J., & Selkoe, D. J. (2002). The amyloid hypothesis of Alzheimer's disease: Progress and problems on the road to therapeutics. *Science (New York, N.Y.)*, *297*(5580), 353-356.

Hebert, L. E., Scherr, P. A., Bienias, J. L., Bennett, D. A., & Evans, D. A. (2003). Alzheimer disease in the US population: Prevalence estimates using the 2000 census. *Archives of Neurology*, *60*(8), 1119-1122.

Higgins, M. E., Davies, J. P., Chen, F. W., & Ioannou, Y. A. (1999). Niemann-Pick C1 is a late endosome-resident protein that transiently associates with

lysosomes and the trans-Golgi network. *Molecular Genetics and Metabolism*, 68(1), 1-13.

Hioki, H., Fujiyama, F., Taki, K., Tomioka, R., Furuta, T., Tamamaki, N., et al. (2003). Differential distribution of vesicular glutamate transporters in the rat cerebellar cortex. *Neuroscience*, 117(1), 1-6.

Honore, T., Drejer, J., Nielsen, M., Watkins, J. C., & Olverman, H. J. (1987). Molecular target size of NMDA antagonist binding sites. *European Journal of Pharmacology*, 136(1), 137-138.

Howland, D. S., Trusko, S. P., Savage, M. J., Reaume, A. G., Lang, D. M., Hirsch, J. D., et al. (1998). Modulation of secreted beta-amyloid precursor protein and amyloid beta-peptide in brain by cholesterol. *The Journal of Biological Chemistry*, 273(26), 16576-16582.

Ishii, K., Tamaoka, A., Mizusawa, H., Shoji, S., Ohtake, T., Fraser, P. E., et al. (1997). Abeta1-40 but not Abeta1-42 levels in cortex correlate with apolipoprotein E epsilon4 allele dosage in sporadic Alzheimer's disease. *Brain Research*, 748(1-2), 250-252.

Iwatsubo, T., Odaka, A., Suzuki, N., Mizusawa, H., Nukina, N., & Ihara, Y. (1994). Visualization of A beta 42(43) and A beta 40 in senile plaques with end-specific A beta monoclonals: Evidence that an initially deposited species is A beta 42(43). *Neuron*, 13(1), 45-53.

Jones, P. H. (2001). Cholesterol: Precursor to many lipid disorders. *The American Journal of Managed Care*, 7(9 Suppl), S289-98.

Kabogo, D., Rauw, G., Amritraj, A., Baker, G., & Kar, S. (2010). Ss-amyloid-related peptides potentiate K⁺-evoked glutamate release from adult rat hippocampal slices. *Neurobiology of Aging*, 31(7), 1164-1172.

Kaila, K. (1994). Ionic basis of GABAA receptor channel function in the nervous system. *Progress in Neurobiology*, 42(4), 489-537.

Karunanithi, S., Marin, L., Wong, K., & Atwood, H. L. (2002). Quantal size and variation determined by vesicle size in normal and mutant drosophila glutamatergic synapses. *The Journal of Neuroscience*, 22(23), 10267-10276.

Kashani, A., Lepicard, E., Poirel, O., Videau, C., David, J. P., Fallet-Bianco, C., et al. (2008). Loss of VGLUT1 and VGLUT2 in the prefrontal cortex is correlated with cognitive decline in alzheimer disease. *Neurobiology of Aging*, 29(11), 1619-1630.

- Kawaguchi, K., Habara, T., Terashima, T., & Kikkawa, S. (2010). GABA modulates development of cerebellar purkinje cell dendrites under control of endocannabinoid signaling. *Journal of Neurochemistry*, *114*(2), 627-638.
- Kirvell, S. L., Esiri, M., & Francis, P. T. (2006). Down-regulation of vesicular glutamate transporters precedes cell loss and pathology in Alzheimer's disease. *Journal of Neurochemistry*, *98*(3), 939-950.
- Kivipelto, M., Helkala, E. L., Laakso, M. P., Hanninen, T., Hallikainen, M., Alhainen, K., et al. (2002). Apolipoprotein E epsilon4 allele, elevated midlife total cholesterol level, and high midlife systolic blood pressure are independent risk factors for late-life alzheimer disease. *Annals of Internal Medicine*, *137*(3), 149-155.
- Kodam, A., Maulik, M., Peake, K., Amritraj, A., Vetrivel, K. S., Thinakaran, G., et al. (2010). Altered levels and distribution of amyloid precursor protein and its processing enzymes in Niemann-Pick type C1-deficient mouse brains. *Glia*, *58*(11), 1267-1281.
- Koudinov, A. R., & Koudinova, N. V. (2001). Essential role for cholesterol in synaptic plasticity and neuronal degeneration. *FASEB Journal*, *15*(10), 1858-1860.
- Kowall, N. W., & Beal, M. F. (1991). Glutamate-, glutaminase-, and taurine-immunoreactive neurons develop neurofibrillary tangles in Alzheimer's disease. *Annals of Neurology*, *29*(2), 162-167.
- Laube, B., Kuhse, J., & Betz, H. (1998). Evidence for a tetrameric structure of recombinant NMDA receptors. *The Journal of Neuroscience*, *18*(8), 2954-2961.
- Lleo, A., Castellvi, M., Blesa, R., & Oliva, R. (2002). Uncommon polymorphism in the presenilin genes in human familial Alzheimer's disease: Not to be mistaken with a pathogenic mutation. *Neuroscience Letters*, *318*(3), 166-168.
- Loftus, S. K., Morris, J. A., Carstea, E. D., Gu, J. Z., Cummings, C., Brown, A., et al. (1997). Murine model of Niemann-Pick C disease: Mutation in a cholesterol homeostasis gene. *Science (New York, N.Y.)*, *277*(5323), 232-235.
- Lujan, R., Shigemoto, R., & Lopez-Bendito, G. (2005). Glutamate and GABA receptor signalling in the developing brain. *Neuroscience*, *130*(3), 567-580.
- Lynch, D. R., & Guttman, R. P. (2001). NMDA receptor pharmacology: Perspectives from molecular biology. *Current Drug Targets*, *2*(3), 215-231.

- Lynch, D. R., & Guttman, R. P. (2002). Excitotoxicity: Perspectives based on N-methyl-D-aspartate receptor subtypes. *The Journal of Pharmacology and Experimental Therapeutics*, 300(3), 717-723.
- Ma, L., Zhao, G., & Xia, F. (2009). Age-related memory decline and the APOE epsilon4 effect. *The New England Journal of Medicine*, 361(20), 1996; author reply 1996-7.
- Macdonald, R. L., & Olsen, R. W. (1994). GABAA receptor channels. *Annual Review of Neuroscience*, 17, 569-602.
- Mahley, R. W. (1988). Apolipoprotein E: Cholesterol transport protein with expanding role in cell biology. *Science (New York, N.Y.)*, 240(4852), 622-630.
- Mancuso, M., Siciliano, G., Filosto, M., & Murri, L. (2006). Mitochondrial dysfunction and Alzheimer's disease: New developments. *Journal of Alzheimer's Disease*, 9(2), 111-117.
- Mano, I., & Teichberg, V. I. (1998). A tetrameric subunit stoichiometry for a glutamate receptor-channel complex. *Neuroreport*, 9(2), 327-331.
- Maulik, M., Ghoshal, B., Kim, J., Wang, Y., Yang, J., Westaway, D., & Kar, S. (2012). Mutant human APP exacerbates pathology in a mouse model of NPC and its reversal by a β -cyclodextrin. *Hum. Mol. Genet.* 21(22), 4857-4875
- McNamara, M. J., Gomez-Isla, T., & Hyman, B. T. (1998). Apolipoprotein E genotype and deposits of Abeta40 and Abeta42 in Alzheimer disease. *Archives of Neurology*, 55(7), 1001-1004.
- Moechars, D., Weston, M. C., Leo, S., Callaerts-Vegh, Z., Goris, I., Daneels, G., et al. (2006). Vesicular glutamate transporter VGLUT2 expression levels control quantal size and neuropathic pain. *The Journal of Neuroscience*, 26(46), 12055-12066.
- Morrison, J. H., & Hof, P. R. (1997a). Life and death of neurons in the aging brain. *Science (New York, N.Y.)*, 278(5337), 412-419.
- Morrison, J. H., & Hof, P. R. (1997b). Life and death of neurons in the aging brain. *Science (New York, N.Y.)*, 278(5337), 412-419.
- Muller, W. E., Mutschler, E., & Riederer, P. (1995). Noncompetitive NMDA receptor antagonists with fast open-channel blocking kinetics and strong voltage-dependency as potential therapeutic agents for Alzheimer's dementia. *Pharmacopsychiatry*, 28(4), 113-124.

Murphy, M. P., Das, P., Nyborg, A. C., Rochette, M. J., Dodson, M. W., Loosbrock, N. M., et al. (2003). Overexpression of nicastrin increases abeta production. *FASEB Journal*, 17(9), 1138-1140.

Murthy, V. N., & Stevens, C. F. (1999). Reversal of synaptic vesicle docking at central synapses. *Nature Neuroscience*, 2(6), 503-507.

Namba, Y., Tomonaga, M., Kawasaki, H., Otomo, E., & Ikeda, K. (1991). Apolipoprotein E immunoreactivity in cerebral amyloid deposits and neurofibrillary tangles in Alzheimer's disease and kuru plaque amyloid in creutzfeldt-jakob disease. *Brain Research*, 541(1), 163-166.

Naureckiene, S., Sleat, D. E., Lackland, H., Fensom, A., Vanier, M. T., Wattiaux, R., et al. (2000). Identification of HE1 as the second gene of Niemann-Pick C disease. *Science (New York, N.Y.)*, 290(5500), 2298-2301.

Nitsch, R. M., Slack, B. E., Wurtman, R. J., & Growdon, J. H. (1992). Release of alzheimer amyloid precursor derivatives stimulated by activation of muscarinic acetylcholine receptors. *Science (New York, N.Y.)*, 258(5080), 304-307.

Obata, K., Hirono, M., Kume, N., Kawaguchi, Y., Itoharu, S., & Yanagawa, Y. (2008). GABA and synaptic inhibition of mouse cerebellum lacking glutamate decarboxylase 67. *Biochemical and Biophysical Research Communications*, 370(3), 429-433.

Ottersen, O. P. (1993). Neurotransmitters in the cerebellum. *Revue Neurologique*, 149(11), 629-636.

Parpura-Gill, A., Beitz, D., & Uemura, E. (1997). The inhibitory effects of beta-amyloid on glutamate and glucose uptakes by cultured astrocytes. *Brain Research*, 754(1-2), 65-71.

Parsons, C. G., Danysz, W., & Quack, G. (1998). Glutamate in CNS disorders as a target for drug development: An update. *Drug News & Perspectives*, 11(9), 523-569.

Pearson, R. C., Esiri, M. M., Hiorns, R. W., Wilcock, G. K., & Powell, T. P. (1985). Anatomical correlates of the distribution of the pathological changes in the neocortex in alzheimer disease. *Proceedings of the National Academy of Sciences of the United States of America*, 82(13), 4531-4534.

Poirier, J., Davignon, J., Bouthillier, D., Kogan, S., Bertrand, P., & Gauthier, S. (1993). Apolipoprotein E polymorphism and Alzheimer's disease. *Lancet*, 342(8873), 697-699.

- Poirier, J., Hess, M., May, P. C., & Finch, C. E. (1991). Astrocytic apolipoprotein E mRNA and GFAP mRNA in hippocampus after entorhinal cortex lesioning. *Brain Research.Molecular Brain Research*, *11*(2), 97-106.
- Pow, D. V., & Robinson, S. R. (1994). Glutamate in some retinal neurons is derived solely from glia. *Neuroscience*, *60*(2), 355-366.
- Price, D. L., Whitehouse, P. J., Struble, R. G., Coyle, J. T., Clark, A. W., DeLong, M. R., et al. (1982). Alzheimer's disease and down's syndrome. *Annals of the New York Academy of Sciences*, *396*, 145-164.
- Refolo, L. M., Malester, B., LaFrancois, J., Bryant-Thomas, T., Wang, R., Tint, G. S., et al. (2000). Hypercholesterolemia accelerates the Alzheimer's amyloid pathology in a transgenic mouse model. *Neurobiology of Disease*, *7*(4), 321-331.
- Reinikainen, K. J., Paljarvi, L., Huuskonen, M., Soininen, H., Laakso, M., & Riekkinen, P. J. (1988). A post-mortem study of noradrenergic, serotonergic and GABAergic neurons in Alzheimer's disease. *Journal of the Neurological Sciences*, *84*(1), 101-116.
- ROBERTS, E., & FRANKEL, S. (1950). Gamma-aminobutyric acid in brain: Its formation from glutamic acid. *The Journal of Biological Chemistry*, *187*(1), 55-63.
- Roberts, R. C., & Difiglia, M. (1988a). Localization of immunoreactive GABA and enkephalin and NADPH-diaphorase-positive neurons in fetal striatal grafts in the quinolinic-acid-lesioned rat neostriatum. *The Journal of Comparative Neurology*, *274*(3), 406-421.
- Roberts, R. C., & Difiglia, M. (1988b). Localization of immunoreactive GABA and enkephalin and NADPH-diaphorase-positive neurons in fetal striatal grafts in the quinolinic-acid-lesioned rat neostriatum. *The Journal of Comparative Neurology*, *274*(3), 406-421.
- Rogaeva, E., Premkumar, S., Song, Y., Sorbi, S., Brindle, N., Paterson, A., et al. (1998). Evidence for an alzheimer disease susceptibility locus on chromosome 12 and for further locus heterogeneity. *The Journal of the American Medical Association*, *280*(7), 614-618.
- Rothman, S. M., & Olney, J. W. (1995). Excitotoxicity and the NMDA receptor--still lethal after eight years. *Trends in Neurosciences*, *18*(2), 57-58.
- Safferling, M., Tichelaar, W., Kummerle, G., Jouppila, A., Kuusinen, A., Keinanen, K., et al. (2001). First images of a glutamate receptor ion channel: Oligomeric state and molecular dimensions of GluRB homomers. *Biochemistry*, *40*(46), 13948-13953.

Samuel, W., Masliah, E., Hill, L. R., Butters, N., & Terry, R. (1994). Hippocampal connectivity and Alzheimer's dementia: Effects of synapse loss and tangle frequency in a two-component model. *Neurology*, *44*(11), 2081-2088.

Schmechel, D. E., Saunders, A. M., Strittmatter, W. J., Crain, B. J., Hulette, C. M., Joo, S. H., et al. (1993). Increased amyloid beta-peptide deposition in cerebral cortex as a consequence of apolipoprotein E genotype in late-onset alzheimer disease. *Proceedings of the National Academy of Sciences of the United States of America*, *90*(20), 9649-9653.

Selkoe, D. J. (2001). Alzheimer's disease: Genes, proteins, and therapy. *Physiological Reviews*, *81*(2), 741-766.

Siman, R., Mistretta, S., Durkin, J. T., Savage, M. J., Loh, T., Trusko, S., et al. (1993). Processing of the beta-amyloid precursor. multiple proteases generate and degrade potentially amyloidogenic fragments. *The Journal of Biological Chemistry*, *268*(22), 16602-16609.

Sisodia, S. S., Koo, E. H., Beyreuther, K., Unterbeck, A., & Price, D. L. (1990). Evidence that beta-amyloid protein in Alzheimer's disease is not derived by normal processing. *Science (New York, N.Y.)*, *248*(4954), 492-495.

Sladeczek, F., Pin, J. P., Recasens, M., Bockaert, J., & Weiss, S. (1985). Glutamate stimulates inositol phosphate formation in striatal neurones. *Nature*, *317*(6039), 717-719.

Sleat, D. E., Wiseman, J. A., El-Banna, M., Price, S. M., Verot, L., Shen, M. M., et al. (2004). Genetic evidence for nonredundant functional cooperativity between NPC1 and NPC2 in lipid transport. *Proceedings of the National Academy of Sciences of the United States of America*, *101*(16), 5886-5891.

Steele, J. E., Palmer, A. M., Stratmann, G. C., & Bowen, D. M. (1989). The N-methyl-D-aspartate receptor complex in Alzheimer's disease: Reduced regulation by glycine but not zinc. *Brain Research*, *500*(1-2), 369-373.

Steinberg, S. J., Mondal, D., & Fensom, A. H. (1996). Co-cultivation of Niemann-Pick disease type C fibroblasts belonging to complementation groups alpha and beta stimulates LDL-derived cholesterol esterification. *Journal of Inherited Metabolic Disease*, *19*(6), 769-774.

Strittmatter, W. J., Weisgraber, K. H., Huang, D. Y., Dong, L. M., Salvesen, G. S., Pericak-Vance, M., et al. (1993). Binding of human apolipoprotein E to synthetic amyloid beta peptide: Isoform-specific effects and implications for late-onset alzheimer disease. *Proceedings of the National Academy of Sciences of the United States of America*, *90*(17), 8098-8102.

- Sucher, N. J., Awobuluyi, M., Choi, Y. B., & Lipton, S. A. (1996). NMDA receptors: From genes to channels. *Trends in Pharmacological Sciences*, 17(10), 348-355.
- Sugiyama, H., Ito, I., & Hirono, C. (1987). A new type of glutamate receptor linked to inositol phospholipid metabolism. *Nature*, 325(6104), 531-533.
- Suzuki, K., Parker, C. C., Pentchev, P. G., Katz, D., Ghetti, B., D'Agostino, A. N., et al. (1995). Neurofibrillary tangles in Niemann-Pick disease type C. *Acta Neuropathologica*, 89(3), 227-238.
- Talbot, C., Lendon, C., Craddock, N., Shears, S., Morris, J. C., & Goate, A. (1994). Protection against Alzheimer's disease with apoE epsilon 2. *Lancet*, 343(8910), 1432-1433.
- Tanabe, Y., Masu, M., Ishii, T., Shigemoto, R., & Nakanishi, S. (1992). A family of metabotropic glutamate receptors. *Neuron*, 8(1), 169-179.
- Tanzi, R. E., Bush, A. I., & Wasco, W. (1994). Genetic studies of Alzheimer's disease: Lessons learned and future imperatives. *Neurobiology of Aging*, 15 Suppl 2, S145-8.
- Tordera, R. M., Totterdell, S., Wojcik, S. M., Brose, N., Elizalde, N., Lasheras, B., et al. (2007). Enhanced anxiety, depressive-like behaviour and impaired recognition memory in mice with reduced expression of the vesicular glutamate transporter 1 (VGLUT1). *The European Journal of Neuroscience*, 25(1), 281-290.
- Tsai, G., Goff, D. C., Chang, R. W., Flood, J., Baer, L., & Coyle, J. T. (1998). Markers of glutamatergic neurotransmission and oxidative stress associated with tardive dyskinesia. *The American Journal of Psychiatry*, 155(9), 1207-1213.
- Uchihara, T., Duyckaerts, C., He, Y., Kobayashi, K., Seilhean, D., Amouyel, P., et al. (1995). ApoE immunoreactivity and microglial cells in Alzheimer's disease brain. *Neuroscience Letters*, 195(1), 5-8.
- Vanier, M. T. (2010). Niemann-Pick disease type C. *Orphanet Journal of Rare Diseases*, 5, 16.
- Vanier, M. T., & Suzuki, K. (1998). Recent advances in elucidating Niemann-Pick C disease. *Brain Pathology (Zurich, Switzerland)*, 8(1), 163-174.
- Vogt, B. A., Crino, P. B., & Volicser, L. (1991). Laminar alterations in gamma-aminobutyric acidA, muscarinic, and beta adrenoceptors and neuron degeneration in cingulate cortex in Alzheimer's disease. *Journal of Neurochemistry*, 57(1), 282-290.

Williams, J. (1997). How does a vesicle know it is full? *Neuron*, 18(5), 683-686.

Wilson, N. R., Kang, J., Hueske, E. V., Leung, T., Varoqui, H., Murnick, J. G., et al. (2005). Presynaptic regulation of quantal size by the vesicular glutamate transporter VGLUT1. *The Journal of Neuroscience*, 25(26), 6221-6234.

Yamaguchi, H., Nakazato, Y., Kawarabayashi, T., Ishiguro, K., Ihara, Y., Morimatsu, M., et al. (1991). Extracellular neurofibrillary tangles associated with degenerating neurites and neuropil threads in alzheimer-type dementia. *Acta Neuropathologica*, 81(6), 603-609.

Yamashita, T., Ishikawa, T., & Takahashi, T. (2003). Developmental increase in vesicular glutamate content does not cause saturation of AMPA receptors at the calyx of held synapse. *The Journal of Neuroscience*, 23(9), 3633-3638.

Zhang, M., Sun, M., Dwyer, N. K., Comly, M. E., Patel, S. C., Sundaram, R., et al. (2003). Differential trafficking of the Niemann-Pick C1 and 2 proteins highlights distinct roles in late endocytic lipid trafficking. *Acta Paediatrica (Oslo, Norway : 1992).Supplement*, 92(443), 63-73; discussion 45.